

Direct Strength Method to Predict the Resistance of Cold-Formed Steel Columns against Local-Distortional Interactive Failure

P.B. Dinis and D. Camotim

**Department of Civil Engineering and Architecture
ICIST, Instituto Superior Técnico
Technical University of Lisbon, Portugal**

Abstract

This paper reports the latest results of an ongoing investigation on the direct strength method (DSM) design of cold-formed steel columns affected by local-distortional interaction, aimed at extending findings unveiled earlier for lipped channels to other cross-section shapes, namely, hat, zed and rack-sections. Following a brief presentation of the most relevant aspects concerning the strength of columns with those cross-section shapes and identical local and distortional buckling stresses, the paper addresses the assembly of a significant column ultimate strength data bank, concerning fixed-ended hat, zed and rack-section columns undergoing strong local-distortional interaction and exhibiting several geometries (cross-section dimensions and lengths) and yield stresses. Then, these ultimate strength data are used to assess the performance of the existing DSM approaches to design columns against local-distortional interactive failures. It is shown that a novel DSM design approach, recently developed or validated in the context of cold-formed steel fixed-ended lipped channel columns affected by local-distortional interaction, can also be successfully applied to hat, zed and rack-section columns under the same circumstances.

Keywords: cold-formed steel columns, local-distortional interaction, lipped channels, hat-sections, zed-sections, rack-sections, ultimate strength, direct strength method.

1 Introduction

Cold-formed steel members invariably display slender thin-walled open cross-sections, making them highly prone to instability phenomena involving cross-section deformation, namely local and distortional buckling – Figures 1(b)-(e) show buckled rack-sections corresponding to column local, distortional and global (flexural-torsional and flexural) buckling modes. Moreover, several commonly used column

geometries (cross-section shape/dimensions and unrestrained length) correspond to similar local (L) and distortional (D) critical buckling stresses, which implies that their post-buckling behaviours (elastic or elastic-plastic), ultimate strengths and failure mechanisms are influenced by the coupling between these two buckling modes (L-D interaction). Indeed, this effect has been thoroughly investigated, both numerically and experimentally, for fixed-ended lipped channel columns (mostly) [1-3] and, very recently, also for fixed-ended hat and zed-section columns [4].

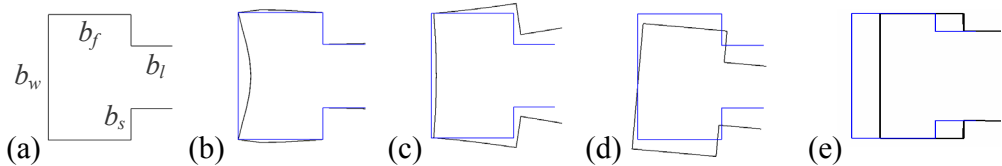


Figure 1: Rack-section (a) geometry and buckled shapes associated with column (b) local, (c) distortional, (d) flexural-torsional and (e) flexural buckling.

Since the structural response and strength of cold-formed steel members is complex and not yet adequately reflected in the current design codes, a fair amount of research has been devoted to develop efficient (safe and economic) design rules for such members. The most relevant fruit of this effort activity was the Direct Strength Method (DSM), which (i) has its roots in the work of Hancock *et al.* [5], (ii) was originally proposed by Schafer and Peköz [6] and (iii) has already been included in the latest versions of the Australian/New Zealand [7] and North American [8] cold-formed steel specifications. The DSM (i) does not require “effective width” calculations and (ii) is currently able of predicting the ultimate strength of columns and beams failing in local, distortional, global and local-global interactive modes. However, as pointed out by Schafer [9], further research is needed before the DSM can be applied with success to members affected by interaction phenomena involving distortional buckling. In the particular case of fixed-ended lipped channel columns experiencing L-D interaction, the authors performed extensive numerical simulations that (i) provided clear evidence that the current DSM local and distortional design curves cannot capture the ultimate strength erosion due to this coupling behaviour and (ii) unveiled features that must appear in a DSM design approach for such members – they were incorporated into a recent proposal of a novel approach [2]. Moreover, the experimental results obtained from column tests reported by various authors [3, 10, 11] also confirmed the ultimate strength erosion stemming from L-D interaction in fixed-ended lipped channel columns.

The aim of the authors’ current research effort is to extend the scope of the DSM-based design approach recently developed for fixed-ended cold-formed steel lipped channel columns [2], by investigating whether it is also applicable to columns exhibiting other cross-section shapes and equally affected by strong L-D interaction.

This design approach adopts “Winter-type” curves and requires knowing (i) the elastic critical (local and distortional) buckling stress, (ii) the critical half-wave length ratio L_{crD}/L_{crL} and (iii) the cross-section elastic/plastic capacity. A first step towards achieving that goal was recently reported in [4], which includes numerical simulations of the post-buckling behaviour and ultimate strength of hat-section and lipped zed-section columns with cross-section dimensions identical to those exhibited by the lipped channel columns analysed earlier (two additional sets of 210 columns each), thus sharing the same local and distortional buckling behaviours. Moreover, these numerical results made it possible to conclude that, as it would be logical to anticipate, the three columns sets behave quite similarly and, in particular, their L-D interactive failure loads are fairly efficiently predicted by the recently proposed DSM-based design approach [2]. Even more recently, the authors [12] began studying also fixed-ended rack-section columns experiencing strong L-D interaction and the outcome of this investigation, which involved 65 columns, indicates that the ultimate strengths of such columns may also be satisfactorily estimated by this novel design approach.

The objectives of this work are (i) to briefly review the DSM-based design approach proposed in [2], (ii) to summarise the findings reported in [4, 12], (iii) to present the results of a parametric study aimed at obtaining a more substantial fixed-ended rack-section column ultimate strength data bank (a total of 195 columns with very close local and distortional buckling stresses are considered), and (iv) to assess whether those ultimate strengths are adequately predicted by the above design approach. As in the previous studies, the numerical column failure loads are obtained by means of ABAQUS [13] shell finite element analyses (SFEA), based on an existing elastic-perfectly plastic model: (i) columns discretised into fine 4-node isoparametric element meshes (length-to-width ratio roughly equal to 1), (ii) fixed-ended conditions modelled by attaching rigid plates to the column end sections and (iii) steel material behaviour described by Prandtl-Reuss’s model – a detailed account of all modelling issues can be found in [14, 15]. The columns analysed exhibit various geometries (all associated with strong L-D interaction) and yield stresses, and contain distortional critical initial imperfections with small amplitudes (10% of the wall thickness).

2 Column Post-Buckling Behaviour and Failure

The main results of recent studies on the elastic-plastic post-buckling behaviour and ultimate strength of fixed cold-formed steel columns strongly affected by L-D interaction [2, 4, 12] are summarised here – the most relevant results obtained for lipped channel (C), hat-section (H), lipped zed-section (Z) and rack-section (R) columns with the cross-section dimensions, lengths and elastic constants given in Figures 2(a₁)-(a₂) are presented and discussed.

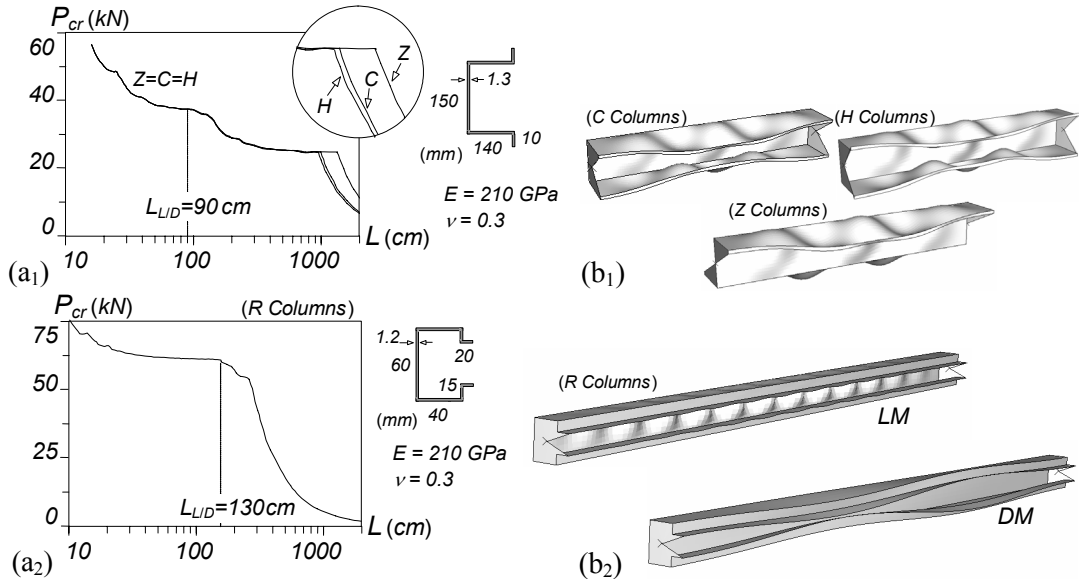


Figure 2: (a) Critical buckling curves and (b) $L_{L/D}$ column buckling modes concerning the (1) C, H, Z and (2) R cross-sections.

The curves shown in Figures 2(a₁)-2(a₂) provide the variation of the ABAQUS critical load P_{cr} with the length L (logarithmic scale), for fixed-ended (i) C, H and Z columns with the same cross-section dimensions (Fig. 2(a₁)), and (ii) R columns (Fig. 2(a₂)). As clearly shown in Figure 2(b₁), the $L_{L/D}=90 \text{ cm}$ C, H and Z columns buckle for $P_{cr}=37.3 \text{ kN}$ (corresponding to $f_{cr}=f_{cr,D}=f_{cr,L}=63.8 \text{ MPa}$) in modes combining arbitrarily (i) a single distortional half-wave and (ii) 5 local half-waves. Similarly, the local and distortional buckling loads of the $L_{L/D}$ rack-section column in Figure 2(a₂) virtually coincide: $P_{cr,D}=60.0 \text{ kN}$ and $P_{cr,L}=60.8 \text{ kN}$ ($f_{cr,D}=285.8 \text{ MPa}$ and $f_{cr,L}=289.6 \text{ MPa}$), associated with buckling modes that combine (i) 24 local and (ii) 2 distortional half-waves (see Fig. 2(b₂)). Obviously, all these $L_{L/D}$ columns have post-buckling behaviours and ultimate strengths strongly affected by L-D interaction.

2.1 Lipped channel, hat-section and zed-section columns

The most relevant results concerning the elastic/perfectly-plastic post-buckling behaviour of fixed-ended C, H and Z columns with the same cross-section dimensions and lengths (sharing a common buckling behaviour) and undergoing L-D interaction are first reported. The columns (i) contain “pure” distortional imperfections with (i₁) inward or outward flange-lip motions (most detrimental initial imperfections, as found in [2, 4]) and (i₂) small amplitudes (10% of the wall thickness t), and (ii) exhibiting three yield-to-critical stress ratios: $f_y/f_{cr} \approx 1.2, 2.4, 3.9$, corresponding to $f_y=75, 150, 250 \text{ MPa}$ ($f_{cr}=f_{cr,L}=f_{cr,D} \approx 63.5 \text{ MPa}$) – for comparative purposes, some elastic results are also shown, which may be viewed as associated with an infinite yield stress (*i.e.*, $f_y=f_{cr}=\infty$).

Figure 3(a) shows the upper portions ($P/P_{cr} > 0.6$) of four equilibrium paths P/P_{cr} vs. v/t , where v is the mid-span top flange-lip corner vertical displacement¹, corresponding to the C columns exhibiting (i) pure inward distortional imperfections and (ii) the three different yield-to-critical stress ratios. As for Figure 3(b), it concerns the column with $f_y/f_{cr} \approx 2.4$ and displays three plastic strain diagrams, corresponding to the equilibrium state locations shown on its equilibrium path, in Figure 3(a), and including the collapse mechanism. On the other hand, Figures 4(a)-(b) show similar elastic-plastic results for H columns with pure outward distortional initial imperfections. Finally, Figures 5(a)-(b) depict similar elastic-plastic results for Z columns also with pure distortional initial imperfections (inward or outward flange-lip motion sense not relevant, since the Z column distortion combines both) – in order to clarify this column plastic strain evolutions, two views per equilibrium state are shown. The observation of all these results makes it possible to conclude that:

- (i) The nature and characteristics of the C, H and Z column elastic-plastic post-buckling behaviours and collapse mechanisms clearly depend on the f_y/f_{cr} value.
- (ii) In the columns with f_y/f_{cr} close to 1.0 (e.g., $f_y/f_{cr} \approx 1.2$), first yielding occurs when the column normal stress distribution is still “fairly uniform” and, thus, precipitates a rather “abrupt” collapse – yielding occurs in a significant portion of the “most deformed (critical) cross-section”, whose location depends on the initial imperfection shape (mid-span, for the columns considered here).
- (iii) In the columns with higher f_y/f_{cr} values (e.g., $f_y/f_{cr} = 2.4, 3.9$), first yielding occurs when the column normal stress distribution is already “heavily non-uniform” and, thus, does not lead to an immediate collapse – instead, collapse occurs after a mild “snap-through” phenomenon, followed by a subsequent strength increase up to a limit point, as is illustrated in Figures 3(a), 4(a) and 5(a).

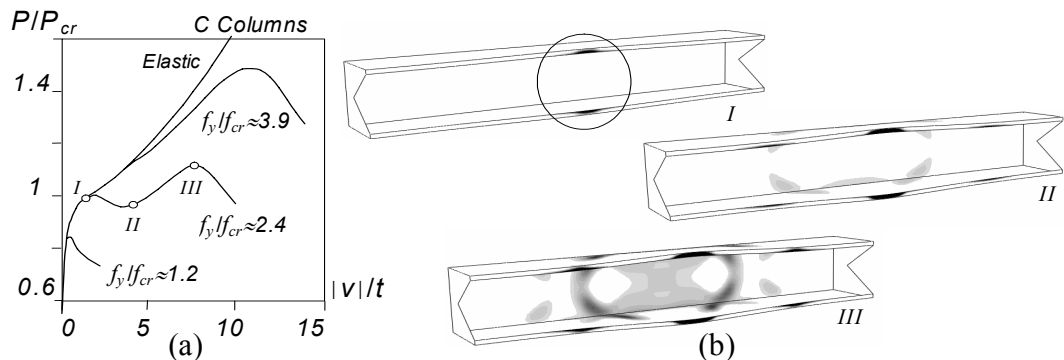


Figure 3: (a) Elastic-plastic P/P_{cr} vs. v/t equilibrium paths ($f_y/f_{cr} \approx 1.2, 2.4, 3.9, \infty$) and (b) plastic strain diagram evolution ($f_y/f_{cr} \approx 2.4$) for C columns with distortional imperfections.

¹ The distinction between the top and bottom flange-lip corner is relevant only for the Z columns, as both flange-lip corners move identically in the C and H columns.

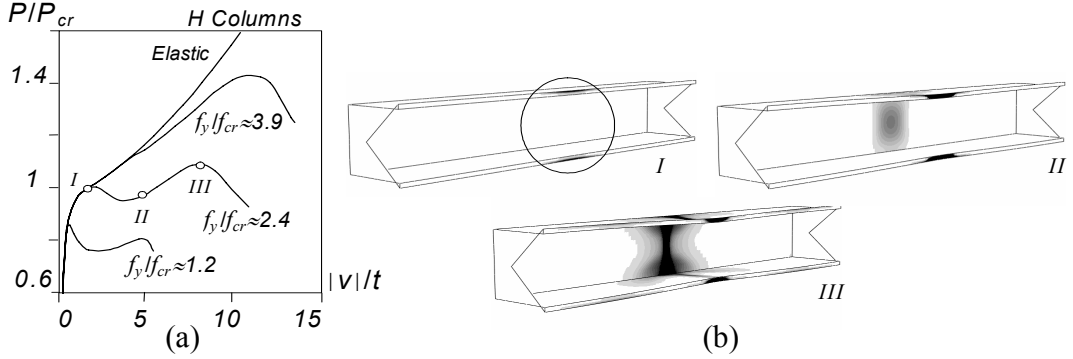


Figure 4: (a) Elastic-plastic P/P_{cr} vs. v/t equilibrium paths ($f_y/f_{cr} \approx 1.2, 2.4, 3.9, \infty$) and (b) plastic strain diagram evolution ($f_y/f_{cr} \approx 2.4$) for H columns with distortional imperfections.

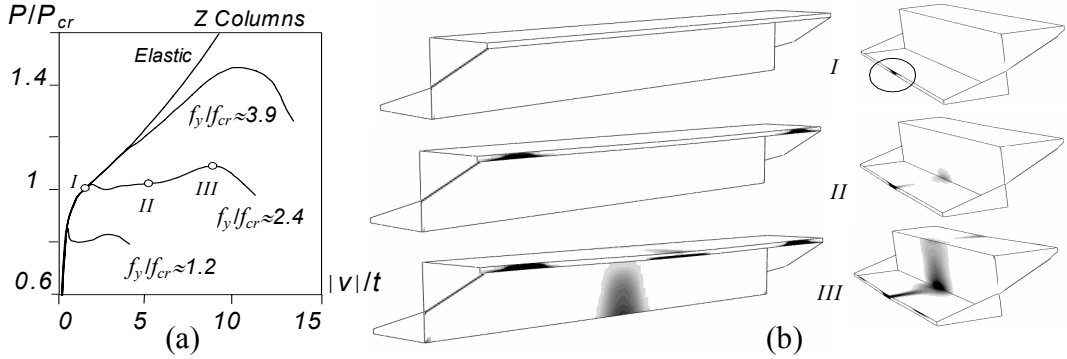


Figure 5: (a) Elastic-plastic P/P_{cr} vs. v/t equilibrium paths ($f_y/f_{cr} \approx 1.2, 2.4, 3.9, \infty$) and (b) plastic strain diagram evolution ($f_y/f_{cr} \approx 2.4$) for Z columns with distortional imperfections.

- (iv) The C, H and Z column yielding patterns and failure mechanisms are quite different: while the first two exhibit symmetry (both flange-lip assemblies are involved), the latter do not (mostly the bottom flange-lip assembly, moving outward, is involved).
- (v) In the C and H columns, (v_1) yielding begins at the two lip free end mid-span zones (see diagrams I in Figs. 3(b) and 4(b)), and (v_2) collapse occurs after the full yielding of the web-flange corner central regions. Note, however, that yielding is more localised in the H columns, where the failure mechanism corresponds to the formation of a well defined “distortional plastic hinge” at mid-span (see diagram III in Fig. 4(b)) – in the C columns yielding spreads along the central $L/3$ segment at failure (see diagram III in Fig. 3(b)).
- (vi) In the Z columns, however, the onset of yielding and failure mechanism involve mostly the mid-span bottom lip, flange and web-flange corner regions, as shown in diagrams I and III of Figure 9(b) – nevertheless, note that yielding also progresses along the top lip regions near the supports prior to collapse, which does not occur in the C and H columns (yielding is restricted to the more or less localised central region).

(vii) In spite of the quite different yielding patterns and failure mechanisms exhibited by the C, H and Z columns, they exhibit very close ultimate loads – Table 1 shows the minute differences between the P_u/P_{cr} values of the three column sets (always below 2%).

Columns	f_y/f_{cr}		
	1.2	2.4	3.9
C	0.84	1.11	1.49
H	0.86	1.09	1.43
Z	0.85	1.09	1.47

Table 1: Variation of P_u/P_{cr} with f_y/f_{cr} for the C, H and Z columns.

2.2 Rack-section columns

This subsection presents and discusses similar results concerning the elastic/perfectly-plastic post-buckling behaviour and failure of fixed-ended rack-section columns experiencing L-D interaction. As before, all the columns analysed (i) contain “pure” distortional initial geometrical imperfections with small amplitudes (maximum flange-stiffener vertical displacement equal to $0.1 t$)² and (ii) exhibit three yield stresses: $f_y = 350, 550, 750 \text{ MPa}$, corresponding to $f_y/f_{cr} \approx 1.2, 1.9, 2.6$ (recall that $f_{cr} = f_{cr,D} \approx 285.8 \text{ MPa}$) – for comparative purposes, some elastic post-buckling results are also shown.

Figure 6(a) shows the upper portions ($P/P_{cr} > 0.6$) of four equilibrium paths P/P_{cr} vs. v/t (v denotes the maximum outward vertical displacement of the top flange-stiffener corner, which occurs at the quarter-span cross-section) concerning R columns with distortional initial imperfections and exhibiting different yield-to-critical stress ratios. As for Figure 6(b), it concerns the column with $f_y/f_{cr} \approx 1.9$ and shows three plastic strain diagrams, corresponding to the equilibrium states indicated on its equilibrium path (see Fig. 6(a)) and including the collapse mechanism – two views for each equilibrium state. The observation of these results prompts the following remarks:

- (i) As in the C, H and Z columns, (i₁) first yielding precipitates the collapse for f_y/f_{cr} values close to 1.0 (e.g., $f_y/f_{cr} \approx 1.2$) and (ii) there is some elastic-plastic strength reserve for higher f_y/f_{cr} values (e.g., for $f_y/f_{cr} \approx 1.9$, there is a 2.9% load increase after first yielding).
- (ii) In the $f_y/f_{cr} \approx 1.9$ column, yielding starts at the stiffener corners in the region close to the most “outwardly distorted” cross-section (see diagram I in Fig. 6(b)). Then, plasticity spreads rapidly to the vertical stiffeners in this region and also begins at the flange-stiffener corners around the most “inwardly distorted” cross-section (see diagram II in Fig. 6(b)). Finally, collapse is precipitated by the full

² The flange-lip motion sense is not relevant because all these column critical distortional buckling modes exhibit even half-wave numbers – see Figure 2(b₂).

yielding of the web-flange corners of the most “inwardly distorted” cross-section, which forms a “distortional plastic hinge” (see diagram *III* in Fig. 6(b)).

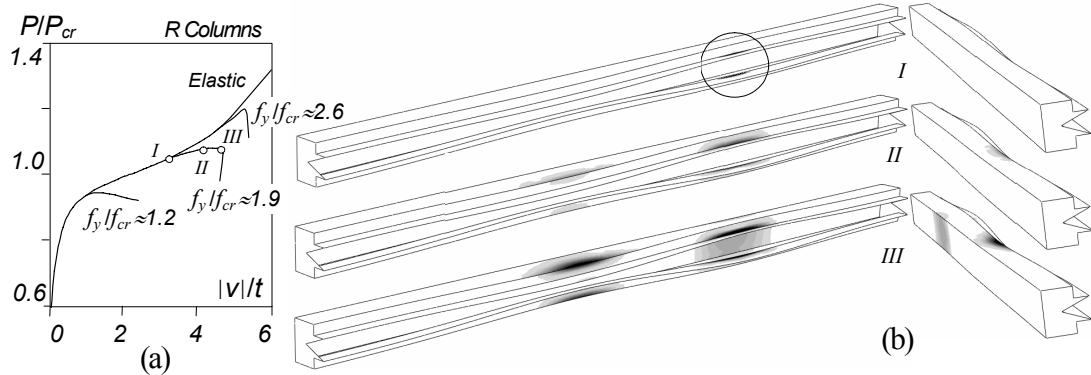


Figure 6: (a) Elastic-plastic P/P_{cr} vs. v/t equilibrium paths ($f_y/f_{cr} \approx 1.2, 1.9, 2.6, \infty$) and (b) plastic strain diagram evolution ($f_y/f_{cr} \approx 1.9$) for R columns with distortional imperfections.

- (iii) Note that the web of the most “inwardly distorted” cross-section (location of the “distortional plastic hinge”) remains practically elastic at collapse. On the other hand, plasticity has already reached the web of the most “outwardly distorted” cross-section (where yielding starts) – see the “back view” of diagram *III* in Figure 6(b).
- (iv) There are visible differences between the equilibrium paths and P_u/P_{cr} values of the analysed R and C, H, Z column sets (at least for the geometries under consideration). First of all, the comparison between Figures 3(a), 4(a), 5(a) and 6(a) reveals that the amount of elastic-plastic strength reserve is considerably smaller for the R columns than for their C, H, Z counterparts. In spite of this fact, for similar f_y/f_{cr} values the R column ultimate load ratios are higher than those of the C, H, Z columns. For instance, for $f_y/f_{cr} \approx 1.2; 2.6$ the R column ultimate load ratios are $P_u/P_{cr} = 0.94; 1.20$, while one has $P_u/P_{cr} = 0.84; 1.11$ (C columns), $P_u/P_{cr} = 0.85; 1.09$ (H columns) and $P_u/P_{cr} = 0.86; 1.09$ (Z columns). One factor possibly contributing to the above differences is the difference in critical buckling mode half-wave numbers (2 for the R columns and 1 for the C, H, Z columns), which leads also to distinct yielding patterns and failure mechanisms.

3 Column Ultimate Strength Data

The objective of the work reported in this section is putting together a failure load data bank concerning cold-formed steel ($E=210$ GPa, $\nu=0.3$) H, Z and R columns experiencing strong L-D interaction (local and distortional critical buckling stresses not more than 10% apart), as was done earlier for C columns [2]. Note that it is

necessary to ensure considerably higher global critical buckling stresses ($f_{cr,G}$), in order to preclude/minimise the occurrence of local-distortion-global coupling effects – previous studies on R columns [16] showed that the closeness of the global critical buckling stress may have a pronounced (detrimental) influence on the column post-buckling behaviour and ultimate strength erosion.

Taking advantage of the fact, illustrated in Figure 2(a₁), that C, H and Z columns sharing the same geometry have identical local and distortional (but not global) buckling stresses, the 14 C column geometries (cross-section dimensions and lengths) identified in [2] as associated with $f_{cr,L} \approx f_{cr,D}$ and much higher global critical buckling stresses ($f_{cr,G}/f_{cr,D} \geq 2.6$) were considered in a parametric study dealing with H and Z columns [4]. Also as done for the C columns, these H and Z column geometries were used as references and slight variations in the flange (b_f), web (b_w) or stiffener (b_s) width generated additional column geometries that exhibit distinct, but fairly close, $f_{cr,L}$ and $f_{cr,D}$ values ($0.90 \leq f_{cr,L}/f_{cr,D} \leq 1.10$). A total of 42 H and Z column geometries were included in the parametric study – just as it had been done before for the C columns [2].

For the R columns, it was necessary to begin again by select the column geometries by means of “trial-and-error” buckling analysis sequences, similarly leading to the identification of 14 “reference geometries”, all associated with $f_{cr,L} \approx f_{cr,D}$ and large enough $f_{cr,G}/f_{cr,D}$ values – note that 6 of these geometries were reported previously [12]. Once more, slight variations of the web, flange, stiffener or lip widths generate column geometries associated with $0.90 \leq f_{cr,L}/f_{cr,D} \leq 1.10$ – a total of 39 R column geometries were identified³.

In order to cover a wide distortional (and local) slenderness $\lambda = (f_y/f_{cr,D})^{0.5}$ range, 5 different yield stresses ($f_y = 150, 250, 350, 550, 750 \text{ MPa}$) are considered for each of the (i) 42 H and Z columns, and (ii) 39 R columns – a total of 210 H, Z column pairs and 195 R columns were analysed, in order to obtain the corresponding ultimate loads. The results were obtained by means of ABAQUS SFEA that neglect the residual stresses and corner effects (both have been shown to have little impact on the column failure loads). Moreover, regardless of the $f_{cr,L}/f_{cr,D}$ value, all columns contained critical-mode distortion initial imperfections with amplitude (maximum top flange-lip corner vertical displacement) equal to 10% of the wall thickness t . Concerning the sense of the flange-lip motions, it was found previously [4, 14, 16] that the most detrimental (lower ultimate strength) are (i) inward, for H and R columns, and (ii) outward, for C columns. At this stage, it is worth recalling that (i) the distinction between top and bottom flange-lip assemblies only is needed in all Z columns, where each distortional half-wave combines one outward and one inward flange-lip assembly motion, and that (ii) the flange-lip motion sense (inward or outward) is not relevant in the C, H and R columns buckling in distortion modes with even half-wave numbers – the same number of half-waves exhibit each of

³ Again, three new column geometries were generated for each reference case, originating a total of 42 R column geometries. However, 3 of them were eliminated because their $f_{cr,G}/f_{cr,D}$ values fell below 1.20 – note that it is fairly difficult to obtain fixed-end R column geometries combining (i) close $f_{cr,L}$ and $f_{cr,D}$ values with (ii) much higher $f_{cr,G}$ values (much more difficult than for C, H, Z columns). The R columns selected in this work exhibit $1.2 \leq f_{cr,G}/f_{cr,D} \leq 2.99$.

them. In the case of C, H and R columns buckling in distortional modes with odd half-wave numbers, the most detrimental flange-lip motion sense obviously applies to the central half-wave.

All fixed-ended column (i) cross-section dimensions (b_w, b_f, b_s, b_l, t) and lengths (L), (ii) critical buckling stresses ($f_{cr,L}, f_{cr,D}, f_{cr,G}$ – evaluated through GBT buckling analyses) and (iii) ultimate stresses f_U are given in Annexes A (H columns), B (Z columns) and C (R columns) – to enable a comparison with the available C column results [2], they are given in Annex D.

4 Column DSM Design against L-D Interactive Failure

The current DSM strength curves for the design of cold formed steel columns are defined by “Winter-type” expressions that (i) were calibrated against fairly large numbers of experimental and/or numerical failure loads and (ii) are able to predict efficiently (safely and accurately) the ultimate strengths of columns failing in local, distortional and global (flexural or flexural-torsional) modes, on the sole basis of elastic buckling and yield stress values – the DSM expressions providing the column nominal strengths against local (f_{NL}), distortional (f_{ND}) and global (f_{NE}) collapses can be found in Schafer’s state-of-the-art report [9]. Moreover, in order to capture also local-global interactive failures, the current DSM replaces f_y by f_{NE} in the f_{NL} expressions, thus providing f_{NLE} estimates. On the other hand, two distinct DSM strategies to estimate the ultimate strength of columns experiencing L-D interaction were also proposed by Hancock *et al.* [5] and Schafer [17]: replacing f_y either (i) by f_{ND} in the f_{NL} equations (NLD approach – f_{NLD}) or (ii) by f_{NL} in the f_{ND} equations (NDL approach – f_{NDL}). Silvestre *et al.* [2] assessed the performance of these two approaches for lipped channel columns and concluded that they provide basically similar results, even if the quality of the f_{NLD} estimates was found to be marginally higher – this explains why this work adopts the NDL approach, defined as

$$f_{NDL} = f_{NL} \quad \text{if} \quad \lambda_D \leq 0.561 \quad , \quad (1)$$

$$f_{NDL} = f_{NL} \left(\frac{f_{cr,D}}{f_{NL}} \right)^{0.6} \left[1 - 0.25 \left(\frac{f_{cr,D}}{f_{NL}} \right)^{0.6} \right] \quad \text{if} \quad \lambda_D > 0.561$$

where $\lambda_D = (f_{NL}/f_{cr,D})^{0.5}$ is the distortional (and local) slenderness – $\lambda_D \equiv \lambda_L \equiv \lambda_{DL}$. Moreover, these authors also showed that the f_{ND} values (i) provide accurate estimates of the column ultimate strengths in the low-to-moderate distortional slenderness range ($\lambda_D < 1.5$), but (ii) perform much worse for more slender columns ($\lambda_D \geq 1.5$). Both these statements are clearly illustrated in Figures 7(a)-(b), showing the variations of f_U/f_{ND} and f_U/f_{NDL} (f_U are the numerical failure loads) with λ_D , and providing the corresponding averages and standard deviations – the quality of an estimate is measured by its closeness to the unit horizontal line.

Silvestre *et al.* [2] went a step further and proposed a novel DSM approach for fixed-ended C columns affected by L-D interaction (NL–D approach – f_{NL-D}). It adopts the current DSM distortional strength curve for $\lambda_D < 1.5$ ($f_{NL-D} = f_{ND}$ ones – no relevant L-D interaction) and, for $\lambda_D \geq 1.5$, proposed a modified local strength f_{NL}^* that (i) depends on the critical half-wave length ratio L_{crD}/L_{crL} (obtained from simply supported column “signature curves”), (ii) leads to f_{ND} and f_{NDL} values if $L_{crD}/L_{crL} \leq 4$ and $L_{crD}/L_{crL} \geq 8$, and (iii) provides column ultimate strength estimates by replacing f_{NL} with f_{NL}^* in (1) – f_{NL}^* is given by the expressions

$$\begin{aligned} f_{NL}^* &= f_y & \text{if} & \frac{L_{crD}}{L_{crL}} \leq 4 \\ f_{NL}^* &= f_y + \left(1 - 0.25 \frac{L_{crD}}{L_{crL}} \right) (f_y - f_{NL}) & \text{if} & 4 < \frac{L_{crD}}{L_{crL}} < 8 \\ f_{NL}^* &= f_{NL} & \text{if} & \frac{L_{crD}}{L_{crL}} \geq 8 \end{aligned} . \quad (2)$$

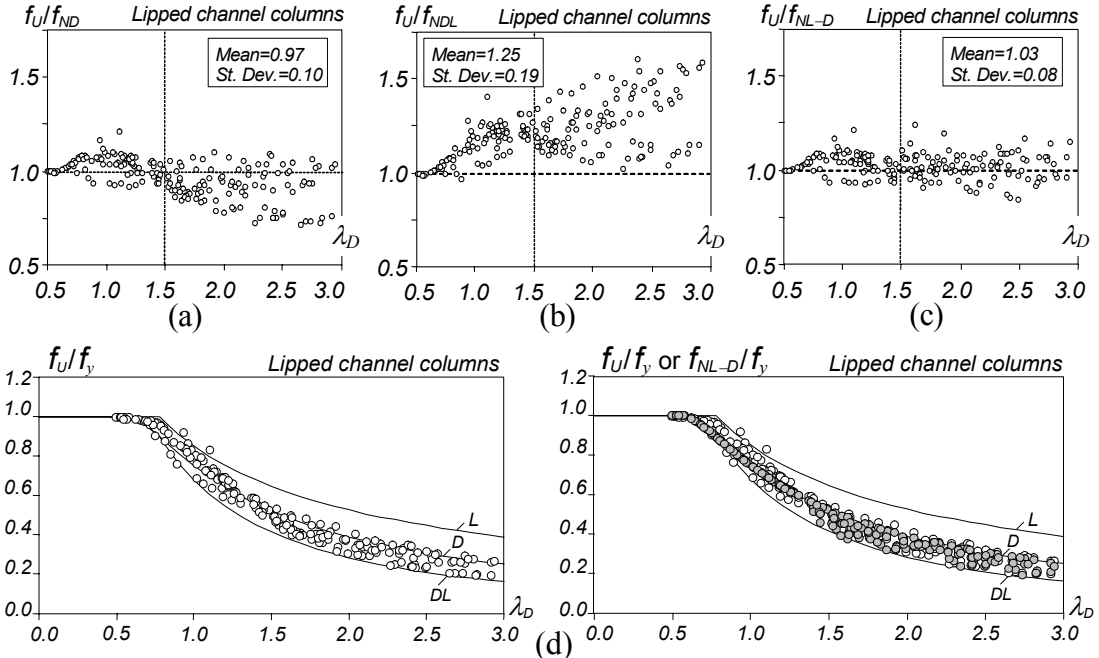


Figure 7: Lipped channel columns: variation with λ_D of the ratios (a) f_U/f_{ND} , (b) f_U/f_{NDL} , (c) f_U/f_{NL-D} and (d) $f_U/f_y + f_{NL-D}/f_y$.

The merits of this new DSM design approach can be assessed by looking at Figures 7(c)-(d), which show the variation, with λ_D , of (i) the f_U/f_{NL-D} values (Fig. 7(c)) and (ii) both the f_U/f_y (white dots) and f_{NL-D}/f_y (grey dots) ratios (Fig. 7(d)) – these figures also include the current DSM strength curves providing the f_{NL}/f_y , f_{ND}/f_y

and f_{NDL}/f_y values (assuming $f_{cr,L}=f_{cr,D}$). These results clearly show that the novel DSM approach provides quite good estimates for the whole set of numerical failure loads: the f_U/f_{NL-D} values have (i) average and standard deviation equal to 1.03 and 0.08, and (ii) a minimum value of 0.84.

The aim of this work is to investigate whether the above novel DSM design approach, developed exclusively in the context of lipped channel columns, is also applicable to cold-formed steel columns exhibiting other cross-section shapes. Therefore, the next sub-sections present and discuss the findings concerning the applicability of this design approach to (i) hat and zed-section columns, and (ii) rack-section columns, all affected by L-D interaction due to very close local and distortional buckling stresses ($f_{cr,L} \approx f_{cr,D} < f_{cr,G}$).

4.1 Hat-section and zed-section columns

As already mentioned, a recent numerical investigation carried out by the authors [4] led to the determination, by means of ABAQUS SFEA, of the ultimate strengths of 210 pairs of fixed-ended H and Z columns with exactly the same cross-section dimensions and lengths as the C columns analysed earlier [2]. These ultimate strength data made it possible to assess the quality of the corresponding DSM estimates and the tables in Annexes A and B include the various column (i) simply supported critical half-wave lengths L_{crL} and L_{crD} (obtained by means of GBT buckling analyses), (ii) three DSM estimates (f_{ND} , f_{NDL} , f_{NL-D}) and (iii) associated numerical-to-predicted ratios. In order to allow a direct comparison with the C column values, the corresponding results are given in the tables presented in Annex D.

Table 2 provides the averages, standard deviations, maximum and minimum values of the C, H and Z column ultimate strength estimates, and Figures 8(a)-(c) plot the variation of the f_{NL-D}/f_U ratio with λ_D for the three column sets (note that Fig. 8(a) is identical to Fig. 7(c)). The observation of the results given in these table and figures leads to the following remarks:

- (i) Given the similar post-buckling and ultimate strength behaviours exhibited by each column trio, it was logical to anticipate an equally similar quality of the f_{NL-D} predictions.
- (ii) Indeed, this was found to be the case: the f_U/f_{NL-D} “clouds” are very similar for the three column sets, as confirmed by the closeness of the corresponding averages and standard deviations: (ii₁) 1.03 and 0.08 (C), (ii₂) 1.03 and 0.07 (H), and (ii₃) 1.04 and 0.08 (Z).
- (iii) Thus, it is fair to conclude that the f_{NL-D} DSM design approach developed in [2] can be readily applied to H and Z columns failing in L-D interactive modes ($f_{cr,L} \approx f_{cr,D}$).

	C Columns			H Columns			Z Columns		
	f_U/f_{ND}	f_U/f_{NDL}	f_U/f_{NL-D}	f_U/f_{ND}	f_U/f_{NDL}	f_U/f_{NL-D}	f_U/f_{ND}	f_U/f_{NDL}	f_U/f_{NL-D}
Average	0.97	1.25	1.03	0.97	1.25	1.03	0.78	1.27	1.04
Standard Deviation	0.15	0.19	0.08	0.09	0.18	0.07	0.15	0.18	0.08
Maximum	1.20	1.83	1.34	1.14	1.82	1.33	1.18	1.85	1.35
Minimum	0.71	0.96	0.84	0.74	0.99	0.87	0.68	0.98	0.88

Table 2: Averages, standard deviations, maximum and minimum values of the C, H and Z column ultimate strength estimates f_{ND} , f_{NDL} and f_{NL-D} .

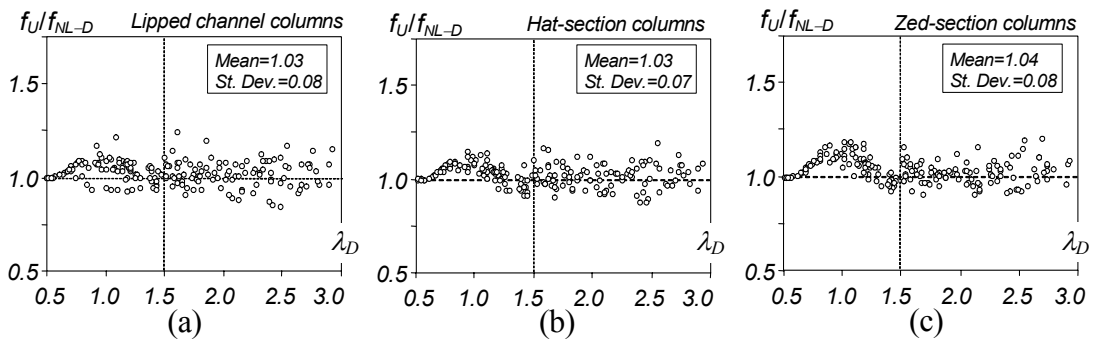


Figure 8: Variation of f_U/f_{NL-D} with λ_D : (a) C columns, (b) H columns and (c) Z columns.

4.2 Rack-section columns

The rack column (i) L_{crL} and L_{crD} values, (ii) DSM ultimate strength estimates f_{ND} , f_{NDL} and f_{NL-D} , and (iii) corresponding numerical-to-predicted ratios are given in the tables in Annex C. Figures 9(a)-(c) plot the variation of their f_{ND}/f_U , f_{NDL}/f_U and f_{NL-D}/f_U ratios with λ_D and show the associated averages and standard deviations – Table 3 provides the averages, standard deviations, maximum and minimum values of those estimates, but separating them for stocky ($\lambda_D < 1.5$) and slender ($\lambda_D \geq 1.5$) columns. On the basis of the observation of the results presented in these figures and table it is possible to conclude that:

- (i) The comparison between the f_U/f_{ND} , f_U/f_{NDL} and f_U/f_{NL-D} value distributions (“clouds”) shown in Figures 9(a)-(c) (R columns) and 7(a)-(c) (C columns) shows that they are qualitatively similar, even if there are a few quantitative discrepancies (e.g., the R column f_{ND} values concerning $\lambda_D < 1.5$ are visibly more conservative than their C column counterparts). This assertion is qualitative confirmed by comparing the values in Tables C1-C3 and D1-D3 (Annexes C and D), and also their averages and standard deviations.
- (ii) The f_U/f_{ND} average and standard deviation are equal to 0.98 and 0.14, with 48 too safe values ($f_U/f_{ND} \geq 1.10$), 47 safe and accurate values ($1.10 < f_U/f_{ND} \leq 1.00$), 48

slightly unsafe values ($1.00 < f_U/f_{ND} \leq 0.90$) and 52 excessively unsafe values ($f_U/f_{ND} \leq 0.90$). However, Figure 9(a) shows that the f_{ND} values are (ii₁) clearly on the safe side (some of them too safe) for $\lambda_D < 1.5$, which indicates little L-D interaction in this slenderness range, and (ii₂) mostly unsafe and inaccurate for $\lambda_D \geq 1.5$ – this can be confirmed by looking at the averages, standard deviations and minimum values given in Table 3, which read as follows: 1.08, 0.07, 0.94 ($\lambda_D < 1.5$) and 0.85, 0.09, 0.62 ($\lambda_D \geq 1.5$). Then the f_{ND} values can be used to predict fairly adequately (a bit conservatively) the failure loads of R columns exhibiting low-to-moderate distortional slenderness, thus extending the DSM design procedure developed earlier, and already shown to be valid for C, H and Z columns, to R columns undergoing L-D interaction.

- (iii) The f_U/f_{ND} average and standard deviation are equal to 1.20 and 0.09, with 161 too safe values, 30 safe and accurate values, and only 4 slightly unsafe values. Figure 9(b) shows that the underestimations occur for both stocky and slender columns, even if the latter exhibit a larger scatter – the standard deviations and maximum values are: 0.07, 1.38 ($\lambda_D < 1.5$) and 0.10, 1.47 ($\lambda_D \geq 1.5$). This was also shown to occur for the C, H and Z columns analysed earlier.
- (iv) The f_U/f_{NL-D} average and standard deviation are equal to 1.11 and 0.11, with 102 too safe values, 65 safe and accurate values, 24 slightly unsafe values, and only 4 overly unsafe values. This means that the quality of the ultimate strength estimates provided by the novel DSM approach is higher than those associated with their f_{ND} and f_{NDL} counterparts (existing DSM approaches). This quality can be felt by looking at Figure 10(b), comparing the numerical f_U/f_y values (white dots) with the corresponding f_{NL-D}/f_y DSM estimates (grey dots). It is clear that the f_{NL-D} values predict the column failure loads quite satisfactorily, even if they are a bit conservative (especially for $\lambda_D \approx 1.0$).
- (v) Although the quality of the R column f_{NL-D} estimates is quite satisfactory, it should be pointed out that it does not reach the level exhibited by their C, H and Z column counterparts. Indeed, the comparison between the f_U/f_{NL-D} values concerning (v₁) the R columns (Fig. 9(c)) and (v₂) the C, H, Z columns (Figs. 8(a)-(c)) shows that the former are considerably more conservative and exhibit a larger scatter – the averages and standard deviations read 1.11, 0.11 (R columns)

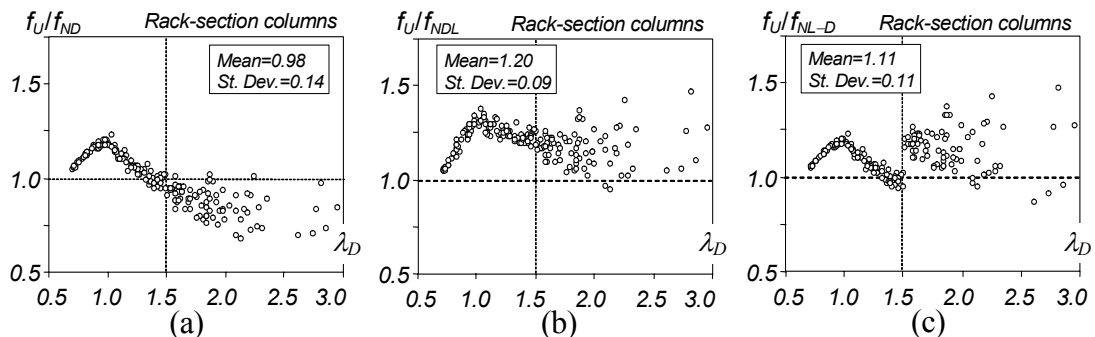


Figure 9: R columns: variation with λ_D of the ratios (a) f_U/f_{ND} , (b) f_U/f_{NDL} and (c) f_U/f_{NL-D} .

	Stocky ($\lambda_D < 1.5$)			Slender ($\lambda_D \geq 1.5$)		
	f_U/f_{ND}	f_U/f_{NDL}	f_U/f_{NL-D}	f_U/f_{ND}	f_U/f_{NDL}	f_U/f_{NL-D}
Average	1.08	1.23	1.08	0.85	1.16	1.14
Standard Deviation	0.07	0.07	0.07	0.09	0.10	0.13
Maximum	1.23	1.38	1.23	1.01	1.47	1.47
Minimum	0.94	1.05	0.94	0.62	0.95	0.78

Table 3: Averages, standard deviations, maximum and minimum values of the R column ultimate strength estimates f_{ND} , f_{NDL} , f_{NL-D} – stocky ($\lambda_D < 1.5$) and slender ($\lambda_D \geq 1.5$) columns.

vs. 1.03, 0.08 (C columns), 1.03, 0.07 (H columns) and 1.04, 0.08 (Z columns). In particular, it is worth noting (v₁) the R column much safer estimates for $\lambda_D \approx 1.0$, (v₂) the considerably higher number of overly safe estimates (102 vs. 23, 27, 44) and (v₃) the clearly more pronounced “vertical dispersion” for $\lambda_D \geq 1.5$ – this dispersion is particularly striking in the higher slenderness range ($\lambda_D \geq 2.6$), in which 4 excessively unsafe estimates (minimum of 0.78) coexist with 6 too conservative estimates (maximum of 1.47).

- (vi) All the unsafe estimates mentioned in the previous item concern columns with global buckling stresses much smaller than the yield stresses ($3.66 \leq f_y/f_{cr,G} \leq 4.99$). This indicates the possible/probable occurrence of an additional interaction phenomenon involving the global (flexural-torsional) buckling mode [16, 18] and further research is necessary in order to investigate how this fact influences the fixed-ended R column post-buckling behaviour and strength – this issue has already been preliminarily addressed by the authors in the context of C columns [19].

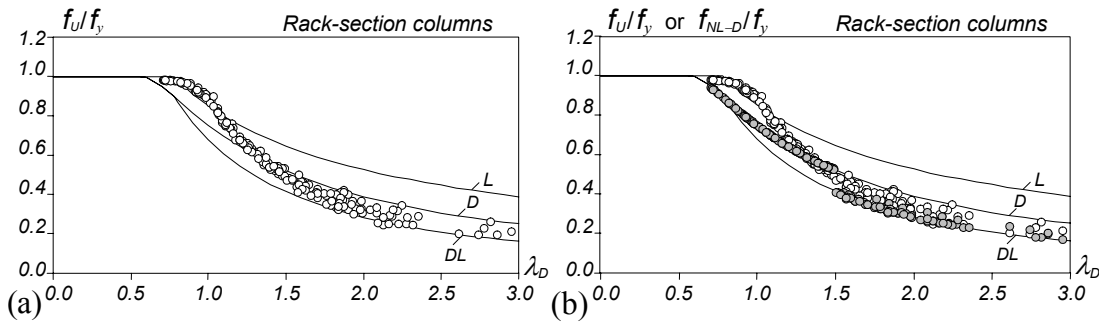


Figure 10: Variation of the (a) f_U/f_y and (b) $f_U/f_y + f_{NL-D}/f_y$ values with λ_D for the R columns.

(vii) The excessively conservative estimates mentioned in item (v) involve exclusively columns that were presented in [12], adopting more crude shell finite element meshes than those considered in this work⁴. It is expected that the adoption of more refined meshes will lower the f_U values by a sizeable amount, thus bringing them in line with those obtained here. Due to time constraints, it is not possible to include the new values in this work – they will be reported in the very near future.

5 Concluding Remarks

This paper reported the latest results of an ongoing investigation on the direct strength method (DSM) design of cold-formed steel fixed-ended columns affected by local-distortion interaction, aimed at extending recent findings obtained for lipped channel columns to other cross-section shapes. After briefly presenting the most relevant aspects concerning the post-buckling and strength behaviour of fixed-ended lipped channel (C), hat-section (H), zed-section (Z) and rack-section (R) columns, the paper (i) summarised findings reported earlier concerning the ultimate strength and DSM design of mostly C, H and Z columns (but also some R columns) and (ii) presented the outcome of a parametric study, carried out by means of ABAQUS shell finite element analyses, aimed at obtaining a more substantial fixed-ended rack-section column ultimate strength data bank (a total of 195 columns have now been considered, instead of the previous 65). Then, the novel DSM-based design approach recently proposed by the authors [2], in the context of C columns, was briefly reviewed and its applicability to H, Z and R columns was investigated.

It was concluded that the application of the above novel DSM-based design approach paper to H, Z and R columns affected by L-D interaction yields generally accurate and mostly safe ultimate strength predictions. In the case of the H and Z columns, whose local and distortional buckling behaviours are very similar to their C column counterparts (with the same cross-section dimensions and lengths), the quality of the DSM ultimate strength estimates is virtually identical to that obtained for the C columns. The picture changed a little in the case of the R columns: although the quality of the estimates is quite satisfactory, it does not reach the level exhibited by their C, H and Z column counterparts, since they are generally more conservative and widely larger scattered⁵.

Finally, a carefully planned experimental program involving 10 tests on rack-section columns exhibiting nearly coincidental distortional and local critical buckling stresses is currently close to completion at The University of Hong Kong. The results of this experimental investigation, to be reported soon, will certainly shed new light on the post-buckling behaviour and strength of rack-section columns

⁴ In fact, these values were really calculated more than four years ago [20].

⁵ Recall that some of the R column ultimate strength values are questionable and will be recalculated in the very near future – the new values are expected to have some impact on the overall quality of the R columns ultimate strength predictions provided by the novel DSM-based design approach.

undergoing strong L-D interaction, thus paving the way for improving their DSM-based design.

References

- [1] N. Silvestre, D. Camotim, P.B. Dinis, "Direct strength prediction of lipped channel columns experiencing local-plate/distortional interaction", *Advanced Steel Construction*, **5**(1), 45-67, 2009.
- [2] N. Silvestre, D. Camotim, P.B. Dinis, "Post-buckling behaviour and direct strength design of lipped channel columns experiencing local/distortional interaction", *Journal of Constructional Steel Research*, **73**(June), 12-30, 2012.
- [3] B. Young, N. Silvestre, D. Camotim, "Cold-formed steel lipped channel columns influenced by local-distortional interaction: strength and DSM design", *Journal of Structural Engineering (ASCE)*, accepted for publication, 2012.
- [4] P.B. Dinis, D. Camotim, R. Fena, "Post-buckling, strength and design of cold-formed steel lipped channel, zed-section and hat-section columns affected by local-distortional interaction", *USB Key Drive Proceedings of SSRC Annual Stability Conference* (Grapevine, 18-21/4), 2012.
- [5] G.J. Hancock, Y.B. Kwon, E.S. Bernard, "Strength design curves for thin-walled sections undergoing distortional buckling", *Journal of Constructional Steel Research*, **31**(2-3), 169-186, 1994.
- [6] B.W. Schafer, T. Pekoz, "Direct strength prediction of cold-formed steel members using numerical elastic buckling solutions", *Thin-Walled Structures - Research and Development* (ICTWS'98 – Singapore, 2-4/12), N. Shanmugam, J.Y.R. Liew, V. Thevendran (eds.), Elsevier, 137-144, 1998.
- [7] Standards of Australia and Standards of New Zealand (AS/NZS), *Cold-Formed Steel Structures* (AS/NZS 4600), Sydney-Wellington, 2005.
- [8] American Iron and Steel Institute (AISI), *North American Specification (NAS) for the Design of Cold-Formed Steel Structural Members* (AISI-S100-07), Washington DC, 2007.
- [9] B.W. Schafer, "Review: the Direct Strength Method of cold-formed steel member design", *Journal of Constructional Steel Research*, **64**(7-8), 766-778, 2008.
- [10] D. Yang, G.J. Hancock, "Compression tests of high strength steel columns with interaction between local and distortional buckling", *Journal of Structural Engineering (ASCE)*, **130**(12), 1954-1963, 2004.
- [11] Y.B. Kwon, B.S. Kim, G.J. Hancock, "Compression tests of high strength cold-formed steel channels with buckling interaction", *Journal of Constructional Steel Research*, **65**(2), 278-289, 2009.
- [12] P.B. Dinis, D. Camotim, R. Fena, "On the DSM design of cold-formed steel columns against local-distortional interactive failure", *Proceedings of Tenth International Conference on Steel Concrete Composite and Hybrid Structures* (ASCCS 2012 – Singapore, 2-4/7), in press, 2012.

- [13] Simulia Inc., ABAQUS Standard (vrs. 6.7-5), 2008.
- [14] P.B. Dinis, D. Camotim, N. Silvestre, “FEM-based analysis of the local-plate /distortional mode interaction in cold-formed steel lipped channel columns”, *Computers & Structures*, **85**(19-20), 1461-1474, 2007.
- [15] P.B. Dinis, D. Camotim, “On the shell finite element buckling and post-buckling analysis of cold-formed steel members”, submitted for publication, 2012.
- [16] P.B. Dinis, D. Camotim, “Local/distortional/global buckling mode interaction in cold-formed steel rack-section columns”, *Proceedings of SSRC Annual Stability Conference* (Orlando, 11-15/5), 481-504, 2010.
- [17] B.W. Schafer, “Local, distortional and Euler buckling in thin-walled columns”, *Journal of Structural Engineering* (ASCE), **128**(3), 289-299, 2002.
- [18] P.B. Dinis, D. Camotim, E. Batista; E. Santos, “Local/distortional/global Mode Coupling in Fixed Lipped Channel Columns: Behaviour and Strength”, *Advanced Steel Construction – an International Journal*, **7**(4), 113-130, 2011.
- [19] P.B. Dinis, N. Silvestre, D. Camotim, “On the relevance of local/distortional interaction in the post-buckling behaviour and strength of cold-formed steel lipped channel columns”, *Proceedings of Twelfth International Conference on Civil, Structural and Environmental Engineering Computing* (CC 2009 – Funchal, 1-4/9), B. Topping, L.C. Neves, R.C. Barros (eds.), Civil-Comp Press (Stirling), paper 22, 2009. (full paper in *CD-ROM Proceedings*)
- [20] N. Silvestre, P.B. Dinis, D. Camotim, “DSM design against Local/Distortional interactive buckling in fixed rack-section columns experiencing multiple wave mode interaction”, *Proceedings of 5th European Conference on Steel and Composite Structures* (EUROSTEEL 2008 – Graz, 3-5/9), R. Ofner, D. Beg, J. Fink, R. Greiner, H. Unterweger (eds.), 1569-1574 (vol. B), 2008.

Appendix A

		L	GBT					SFEA		DSM						
			L _{crL}	L _{crD}	f _{crL}	f _{crD}	f _{crG}	f _y	f _u	λ _D	f _{ND}	f _{NDL}	f _{NL-D}	f _{U/f_{ND}}	f _{NDL/f_U}	f _{NL-D/f_U}
<i>b_w=100; b_r=100; t=1.9mm</i>	<i>b_s=17.5</i>	1760	100	745	262.2	262.2	471.7	150	145	0.76	136	136	136	1.06	1.06	1.06
								250	213	0.98	191	174	191	1.11	1.22	1.11
								350	245	1.16	232	200	232	1.05	1.22	1.05
								550	275	1.45	296	237	296	0.93	1.16	0.93
	<i>b_s=20</i>	1760	100	815	262.9	284.6	457.7	150	147	0.73	139	139	139	1.05	1.05	1.05
								250	225	0.94	197	180	197	1.14	1.25	1.14
								350	274	1.11	241	207	241	1.14	1.32	1.14
								550	298	1.39	308	246	308	0.97	1.21	0.97
	<i>b_s=16</i>	1760	100	700	261.5	243.4	481.1	150	142	0.79	134	134	134	1.06	1.06	1.06
								250	203	1.01	185	170	185	1.09	1.20	1.09
								350	228	1.20	225	194	225	1.01	1.17	1.01
								550	269	1.50	286	229	245	0.94	1.17	1.10
<i>b_r=80; b_s=10; t=1.0mm</i>	<i>b_w=95</i>	2500	85	595	103.9	103.9	223.0	150	91	1.20	96	82	96	0.95	1.11	0.95
								250	111	1.55	126	99	106	0.88	1.12	1.04
								350	114	1.84	149	111	122	0.77	1.03	0.94
								550	148	2.30	184	128	145	0.81	1.15	1.02
	<i>b_w=88</i>	2500	85	585	114.7	108.2	193.2	150	97	1.18	98	85	98	0.99	1.14	0.99
								250	115	1.52	128	103	111	0.90	1.12	1.04
								350	127	1.80	152	115	127	0.84	1.10	1.00
								550	151	2.25	188	134	151	0.80	1.13	1.00
	<i>b_w=105</i>	2500	90	605	89.0	93.0	267.4	150	94	1.27	91	76	91	1.03	1.24	1.03
								250	103	1.64	119	91	101	0.87	1.13	1.02
								350	108	1.94	140	102	116	0.77	1.06	0.93
								550	128	2.43	173	118	139	0.74	1.08	0.92
<i>b_r=80; b_s=10; t=2.4mm</i>	<i>b_w=114</i>	1150	95	500	172.0	172.0	1451.2	150	126	0.93	119	110	119	1.06	1.14	1.06
								250	162	1.21	160	136	160	1.01	1.19	1.01
								350	190	1.43	191	154	191	0.99	1.23	0.99
								550	234	1.79	240	180	223	0.98	1.30	1.05
	<i>b_w=120</i>	1150	100	505	157.1	167.5	1583.1	150	124	0.95	117	107	117	1.06	1.16	1.06
								250	158	1.22	158	132	158	1.00	1.20	1.00
								350	186	1.45	189	150	189	0.99	1.24	0.99
								550	230	1.81	236	175	222	0.97	1.31	1.03
	<i>b_w=106</i>	1150	90	495	194.4	180.8	1277.4	150	128	0.91	121	115	121	1.06	1.11	1.06
								250	168	1.18	163	142	163	1.03	1.18	1.03
								350	196	1.39	196	161	196	1.00	1.22	1.00
								550	241	1.74	246	189	227	0.98	1.28	1.06
<i>b_w=100; b_s=10; t=1.4mm</i>	<i>b_s=55</i>	620	80	310	589.0	590.8	3342.1	150	150	0.50	150	150	150	1.00	1.00	1.00
								250	248	0.65	243	243	243	1.02	1.02	1.02
								350	341	0.77	315	315	315	1.08	1.08	1.08
	<i>b_s=50</i>	620	80	290	598.1	625.4	3137.1	150	150	0.49	150	150	150	1.09	1.19	1.09
								250	248	0.63	246	246	246	1.01	1.01	1.01
								350	343	0.75	320	320	320	1.07	1.07	1.07
	<i>b_s=60</i>	620	85	325	581.2	558.9	3513.5	150	149	0.52	150	150	150	0.99	0.99	0.99
								250	246	0.67	241	241	241	1.02	1.02	1.02
								350	333	0.79	310	310	310	1.07	1.07	1.07

Table A1: H columns – SFEA ultimate strengths and DSM estimates (dimensions in mm, stresses in MPa) – I

		GBT					SFEA		DSM							
	L	L _{crL}	L _{crD}	f _{crL}	f _{crD}	f _{crG}	f _y	f _U	λ _D	f _{ND}	f _{NDL}	f _{NL-D}	f _{U/f_{ND}}	f _{NDL/f_U}	f _{NL-D/f_U}	
<i>b_w=180; b_s=10; t=1.9mm</i>	<i>b_f=110</i>	1030	150	590	113.1	113.1	4401.6	150	104	1.15	100	86	100	1.04	1.21	1.04
								250	133	1.49	131	104	131	1.01	1.27	1.01
								350	158	1.76	155	117	155	1.02	1.35	1.02
								550	198	2.21	192	136	192	1.03	1.45	1.03
								750	233	2.58	222	150	222	1.05	1.55	1.05
	<i>b_f=130</i>	1030	160	655	108.8	100.0	4735.7	150	94	1.22	95	81	95	0.99	1.16	0.99
								250	120	1.58	123	98	123	0.97	1.23	0.98
								350	143	1.87	146	110	145	0.98	1.30	0.99
								550	181	2.35	180	127	179	1.01	1.42	1.01
<i>b_w=180; b_s=20; t=4.0mm</i>	<i>b_f=90</i>	1030	145	515	116.4	124.3	3883.1	150	114	1.10	104	90	104	1.10	1.27	1.10
								250	147	1.42	137	109	137	1.07	1.34	1.07
								350	160	1.68	163	123	163	0.98	1.30	0.98
								550	219	2.10	202	143	202	1.08	1.53	1.08
								750	254	2.46	233	158	233	1.09	1.60	1.09
	<i>b_f=100</i>	2000	145	620	501.5	510.9	1044.6	150	150	0.54	150	150	150	1.00	1.00	1.00
								250	247	0.70	237	237	237	1.04	1.04	1.04
								350	329	0.83	301	292	301	1.09	1.13	1.09
								550	412	1.04	400	356	400	1.03	1.16	1.03
<i>b_w=110; b_f=85; t=2.4mm</i>	<i>b_s=15</i>	940	95	545	458.8	471.5	1947.2	150	150	0.52	150	150	150	1.00	1.00	1.00
								250	248	0.67	241	241	241	1.03	1.03	1.03
								350	338	0.79	309	300	309	1.09	1.13	1.09
								550	448	1.00	414	368	414	1.08	1.22	1.08
								750	512	1.16	495	418	495	1.03	1.23	1.03
	<i>b_f=110</i>	2000	150	660	494.4	463.8	1099.3	150	149	0.57	150	150	150	0.99	0.99	0.99
								250	244	0.73	231	231	231	1.06	1.06	1.06
								350	313	0.87	292	282	292	1.07	1.11	1.07
								550	392	1.09	384	342	384	1.02	1.15	1.02
<i>b_w=100; b_s=5; t=1.0mm</i>	<i>b_f=50</i>	1400	80	275	104.4	107.2	658.2	150	148	0.56	150	150	150	0.99	0.99	0.99
								250	240	0.73	232	232	232	1.03	1.03	1.03
								350	305	0.86	293	279	293	1.04	1.09	1.04
								550	393	1.08	387	339	387	1.02	1.16	1.02
								750	447	1.26	460	383	460	0.97	1.17	0.97
	<i>b_f=45</i>	1400	80	250	105.6	121.6	606.4	150	148	0.61	149	149	149	1.00	1.00	1.00
								250	233	0.79	222	222	222	1.05	1.05	1.05
								350	287	0.94	276	263	276	1.04	1.09	1.04
								550	374	1.17	360	317	360	1.04	1.18	1.04
<i>b_w=100; b_s=5; t=1.0mm</i>	<i>b_f=55</i>	1400	85	290	103.1	97.3	701.4	150	149	0.55	150	150	150	0.99	0.99	0.99
								250	244	0.71	235	235	235	1.04	1.04	1.04
								350	322	0.84	299	285	299	1.08	1.13	1.08
								550	446	1.05	397	347	397	1.12	1.28	1.12
								750	500	1.22	473	393	473	1.06	1.27	1.06

Table A2: H columns – SFEA ultimate strengths and DSM estimates (dimensions in mm, stresses in MPa) – II

	L	GBT					SFEA			DSM						
		L _{crL}	L _{crD}	f _{crL}	f _{crD}	f _{crG}	f _y	f _U	λ _D	f _{ND}	f _{NDL}	f _{NL-D}	f _U /f _{ND}	f _{NDL} /f _U	f _{NL-D} /f _U	
<i>b_w=80; b_s=10; t=1.3mm</i>	<i>b_w=115</i>	2400	95	540	126.8	128.6	342.0	150	110	1.08	106	93	106	1.04	1.19	1.04
								250	131	1.39	140	113	140	0.94	1.16	0.94
								350	145	1.65	166	127	151	0.88	1.14	0.96
								550	169	2.07	206	148	184	0.82	1.14	0.92
								750	184	2.41	238	164	211	0.77	1.13	0.87
<i>b_w=80; b_s=10; t=0.95mm</i>	<i>b_w=100</i>	2400	90	530	137.0	132.0	267.9	150	112	1.07	107	95	107	1.05	1.18	1.05
								250	133	1.38	141	116	141	0.94	1.15	0.94
								350	152	1.63	168	131	152	0.91	1.16	1.00
								550	176	2.04	209	152	185	0.84	1.16	0.95
								750	191	2.38	241	168	211	0.79	1.14	0.91
<i>b_w=125</i>	<i>b_w=125</i>	2400	105	545	109.2	123.7	128.5	150	104	1.10	104	89	104	1.00	1.17	1.00
								250	125	1.42	137	108	137	0.91	1.16	0.91
								350	144	1.68	162	121	152	0.89	1.19	0.95
								550	171	2.11	202	141	186	0.85	1.21	0.92
								750	187	2.46	233	156	214	0.80	1.20	0.87
<i>b_w=95; b_s=10; t=0.95mm</i>	<i>b_s=10</i>	2500	85	610	93.8	94.2	222.6	150	92.6	1.26	92	77	92	1.01	1.20	1.01
								250	106	1.63	120	93	99	0.88	1.14	1.07
								350	118	1.93	141	104	113	0.84	1.14	1.05
								550	145	2.42	174	120	134	0.83	1.21	1.08
								750	155	2.82	200	132	150	0.77	1.17	1.03
<i>b_w=95; b_s=9; t=0.95mm</i>	<i>b_s=9</i>	2500	85	570	93.6	89.0	226.1	150	83.8	1.30	90	75	90	0.94	1.12	0.94
								250	101	1.68	116	90	100	0.87	1.12	1.01
								350	113	1.98	137	101	114	0.82	1.12	0.99
								550	136	2.49	169	117	137	0.80	1.17	1.00
								750	144	2.90	194	128	154	0.74	1.12	0.94
<i>b_w=95; b_s=11; t=0.95mm</i>	<i>b_s=11</i>	2500	85	655	94.0	100.1	219.1	150	101	1.22	95	79	95	1.07	1.28	1.07
								250	113	1.58	124	95	98	0.91	1.19	1.16
								350	123	1.87	146	107	110	0.84	1.15	1.11
								550	142	2.34	180	124	129	0.79	1.15	1.10
								750	161	2.74	207	136	143	0.78	1.18	1.12
<i>b_w=150; b_s=10; t=1.2mm</i>	<i>b_s=140</i>	1430	145	835	53.8	53.8	1804.5	150	63	1.67	70	54	64	0.90	1.17	0.99
								250	82	2.16	90	64	80	0.92	1.28	1.03
								350	99	2.55	105	71	92	0.95	1.39	1.08
								550	125	3.20	128	81	111	0.98	1.54	1.13
								750	148	3.73	146	89	126	1.01	1.66	1.18
<i>b_w=150; b_s=10; t=1.2mm</i>	<i>b_s=130</i>	1430	140	795	57.4	59.0	1777.4	150	65	1.59	73	57	67	0.89	1.15	0.97
								250	86	2.06	94	68	84	0.92	1.28	1.02
								350	104	2.44	110	75	97	0.95	1.38	1.07
								550	132	3.05	135	86	118	0.98	1.53	1.12
								750	155	3.57	154	95	134	1.00	1.64	1.16
<i>b_w=150; b_s=10; t=1.2mm</i>	<i>b_s=150</i>	1430	155	870	51.1	48.9	1824.9	150	59	1.75	67	51	61	0.88	1.15	0.96
								250	77	2.26	85	60	76	0.91	1.28	1.01
								350	92	2.68	99	67	88	0.93	1.38	1.05
								550	118	3.35	121	77	106	0.97	1.54	1.11
								750	139	3.92	139	84	121	1.00	1.66	1.15
<i>b_w=200; b_s=10; t=1.5mm</i>	<i>b_s=12.5</i>	1850	200	1105	46.1	46.1	1931.2	150	58	1.80	65	49	59	0.90	1.20	0.98
								250	76	2.33	82	57	74	0.92	1.32	1.02
								350	92	2.76	96	64	86	0.96	1.44	1.08
								550	117	3.45	117	73	103	1.00	1.60	1.13
								750	137	4.03	134	80	118	1.02	1.71	1.17
<i>b_w=200; b_s=10; t=1.5mm</i>	<i>b_s=14</i>	1850	195	1200	45.6	38.3	1915.2	150	58	1.98	59	44	52	0.98	1.30	1.11
								250	76	2.55	75	52	64	1.02	1.45	1.19
								350	91	3.02	87	58	73	1.05	1.57	1.25
								550	112	3.79	106	66	87	1.06	1.70	1.28
								750	131	4.43	121	72	99	1.09	1.82	1.33
<i>b_w=200; b_s=10; t=1.5mm</i>	<i>b_s=11</i>	1850	205	1010	46.5	52.8	1946.1	150	59	1.69	69	52	66	0.85	1.14	0.90
								250	76	2.18	89	62	83	0.86	1.24	0.91
								350	90	2.57	103	68	97	0.87	1.31	0.93
								550	116	3.23	127	79	118	0.92	1.48	0.98
								750	135	3.77	145	86	134	0.93	1.57	1.00

Table A3: H columns – SFEA ultimate strengths and DSM estimates (dimensions in mm, stresses in MPa) – III

		L	GBT					SFEA		DSM						
			L _{crL}	L _{crD}	f _{crL}	f _{crD}	f _{crG}	f _y	f _U	λ _D	f _{ND}	f _{NDL}	f _{NL-D}	f _{U/f_{ND}}	f _{NDL/f_U}	f _{NL-D/f_U}
<i>b_w=235; b_r=160; t=1.9mm</i>	<i>b_s=12.5</i>	1950	200	910	64.5	65.3	2206.9	150	76	1.52	77	61	75	0.99	1.25	1.01
								250	99	1.96	99	73	96	1.00	1.37	1.03
								350	117	2.32	116	81	112	1.01	1.45	1.04
								550	144	2.90	142	93	137	1.01	1.55	1.05
<i>b_w=150; b_s=10; t=1.9mm</i>	<i>b_s=14</i>	1950	200	985	64.2	56.3	2191.6	150	73	1.63	72	57	69	1.01	1.28	1.06
								250	80	2.11	92	67	87	0.87	1.19	0.92
								350	111	2.49	107	75	101	1.04	1.48	1.10
								550	142	3.13	131	86	123	1.08	1.65	1.16
<i>b_w=150; b_s=11</i>	<i>b_s=11</i>	1950	200	830	64.7	74.9	2220.6	150	78	1.42	83	65	83	0.95	1.21	0.95
								250	100	1.83	107	78	106	0.94	1.29	0.95
								350	119	2.16	125	87	124	0.95	1.37	0.96
								550	150	2.71	154	100	152	0.98	1.50	0.99
<i>b_w=150; b_s=10; t=1.9mm</i>	<i>b_r=140</i>	900	150	800	63.6	63.6	4553.5	150	69	1.54	76	60	71	0.91	1.15	0.97
								250	89	1.98	98	71	90	0.91	1.25	0.99
								350	108	2.35	115	80	105	0.94	1.36	1.03
								550	137	2.94	140	92	127	0.98	1.50	1.08
<i>b_w=150; b_s=10; t=1.9mm</i>	<i>b_r=130</i>	900	140	760	67.9	71.6	4484.8	150	73	1.45	81	64	81	0.91	1.14	0.91
								250	96	1.87	104	77	95	0.92	1.25	1.00
								350	114	2.21	122	85	111	0.93	1.33	1.03
								550	144	2.77	150	98	135	0.96	1.46	1.07
<i>b_w=150; b_s=10; t=1.9mm</i>	<i>b_r=150</i>	900	155	835	58.3	58.3	4605.1	150	66	1.60	73	57	68	0.90	1.16	0.97
								250	85	2.07	93	67	86	0.91	1.26	0.99
								350	96	2.45	109	75	99	0.88	1.28	0.97
								550	131	3.07	134	86	120	0.98	1.52	1.09

Table A4: H columns – SFEA ultimate strengths and DSM estimates (dimensions in mm, stresses in MPa) – IV

Appendix B

		GBT					SFEA		DSM							
		L	L _{crL}	L _{crD}	f _{crL}	f _{crD}	f _{crG}	f _y	f _u	λ _D	f _{ND}	f _{NDL}	f _{NL-D}	f _{U/f_{ND}}	f _{NDL/f_U}	f _{NL-D/f_U}
<i>b_w=100; b_r=10; t=2.4mm</i>	<i>b_r=55</i>	620	85	305	583.3	563.4	5112.8	150	149	0.52	150	150	150	0.99	0.99	0.99
			250	246	0.67	241	241	241	241	1.02	1.02	1.02	1.08	1.08	1.08	
			350	336	0.79	311	311	311	311	1.08	1.08	1.08	1.11	1.11	1.11	
			550	463	0.99	416	381	416	416	1.11	1.11	1.11	1.21	1.21	1.21	
	<i>b_r=50</i>	620	80	285	589.5	599.8	4456.4	150	149	0.50	150	150	150	0.99	0.99	0.99
			250	247	0.65	244	244	244	244	1.01	1.01	1.01	1.07	1.07	1.07	
			350	339	0.76	317	317	317	317	1.07	1.07	1.07	1.12	1.12	1.12	
			550	476	0.96	427	391	427	427	1.12	1.12	1.12	1.22	1.22	1.22	
	<i>b_r=60</i>	620	85	325	578.9	528.9	5751.9	150	149	0.53	150	150	150	0.99	0.99	0.99
			250	245	0.69	238	238	238	238	1.03	1.03	1.03	1.08	1.08	1.08	
			350	330	0.81	305	304	305	305	1.08	1.08	1.08	1.11	1.11	1.11	
			550	450	1.02	406	372	406	406	1.11	1.11	1.11	1.21	1.21	1.21	
<i>b_w=180; b_r=10; t=1.9mm</i>	<i>b_r=110</i>	1030	150	585	112.9	123.8	6379.8	150	104	1.10	104	89	104	1.00	1.17	1.00
			250	132	1.42	137	109	137	137	0.96	0.96	0.96	1.22	1.22	0.96	
			350	157	1.68	162	122	162	162	0.97	0.97	0.97	1.28	1.28	0.97	
			550	197	2.11	202	142	202	202	0.98	0.98	0.98	1.38	1.38	0.98	
	<i>b_r=130</i>	1030	160	655	108.5	98.8	7922.1	150	95	1.23	94	81	94	1.01	1.18	1.01
			250	120	1.59	123	97	122	122	0.98	0.98	0.98	1.23	1.23	0.98	
			350	143	1.88	145	109	144	144	0.99	0.99	0.99	1.31	1.31	0.99	
			550	182	2.36	179	126	178	178	1.02	1.02	1.02	1.44	1.44	1.02	
	<i>b_r=90</i>	1030	145	510	116.0	147.2	4723.2	150	116	1.01	112	96	112	1.04	1.21	1.04
			250	145	1.30	149	118	149	149	0.97	0.97	0.97	1.23	1.23	0.97	
			350	178	1.54	177	133	177	177	1.00	1.00	1.00	1.34	1.34	1.00	
			550	225	1.93	221	155	221	221	1.02	1.02	1.02	1.45	1.45	1.02	
<i>b_w=110; b_r=100; t=1.9mm</i>	<i>b_s=17.5</i>	1760	105	755	261.9	264.1	1424.0	150	145	0.75	137	137	137	1.06	1.06	1.06
			250	212	0.97	192	175	192	192	1.11	1.11	1.11	1.21	1.21	1.11	
			350	246	1.15	233	201	233	233	1.06	1.06	1.06	1.23	1.23	1.06	
			550	280	1.44	297	238	297	297	0.94	0.94	0.94	1.18	1.18	0.94	
	<i>b_s=20</i>	1760	105	825	262.7	307.8	1455.4	150	145	0.70	142	142	142	1.02	1.02	1.02
			250	218	0.90	203	185	203	203	1.07	1.07	1.07	1.18	1.18	1.07	
			350	264	1.07	249	213	249	249	1.06	1.06	1.06	1.24	1.24	1.06	
			550	302	1.34	320	255	320	320	0.94	0.94	0.94	1.19	1.19	0.94	
	<i>b_s=16</i>	1760	105	710	261.1	240.6	1405.6	150	143	0.79	133	133	133	1.07	1.07	1.07
			250	201	1.02	185	169	185	185	1.09	1.09	1.09	1.19	1.19	1.09	
			350	239	1.21	224	193	224	224	1.07	1.07	1.07	1.24	1.24	1.07	
			550	270	1.51	284	228	247	247	0.95	0.95	0.95	1.18	1.18	1.09	
<i>b_r=80; b_s=10; t=1.0mm</i>	<i>b_w=95</i>	2500	85	595	103.8	103.9	468.2	150	97	1.20	96	82	96	1.00	1.18	1.00
			250	112	1.55	126	99	106	106	0.89	0.89	0.89	1.13	1.13	1.05	
			350	122	1.84	149	111	122	122	0.82	0.82	0.82	1.10	1.10	1.00	
	<i>b_w=88</i>	2500	85	585	114.6	107.2	432.5	150	99	1.18	98	84	98	1.01	1.17	1.01
			250	117	1.53	128	102	110	110	0.92	0.92	0.92	1.15	1.15	1.06	
			350	126	1.81	151	115	126	126	0.83	0.83	0.83	1.10	1.10	1.00	
	<i>b_w=105</i>	2500	90	600	88.9	99.4	512.9	150	93	1.23	94	78	94	0.98	1.19	0.98
			250	109	1.59	123	94	105	105	0.89	0.89	0.89	1.16	1.16	1.04	
			350	122	1.88	145	105	121	121	0.84	0.84	0.84	1.16	1.16	1.01	
			550	145	2.35	179	122	145	145	0.81	0.81	0.81	1.19	1.19	1.00	
			750	167	2.75	207	135	163	163	0.81	0.81	0.81	1.24	1.24	1.02	

Table B1: Z columns – SFEA ultimate strengths and DSM estimates (dimensions in mm, stresses in MPa) – I

		GBT					SFEA		DSM							
	L	L _{crL}	L _{crD}	f _{crL}	f _{crD}	f _{crG}	f _y	f _U	λ _D	f _{ND}	f _{NDL}	f _{NL-D}	f _U /f _{ND}	f _{NDL} /f _U	f _{NL-D} /f _U	
$b_f=80; b_s=10; t=1.5mm$	$b_w=114$	1150	95	500	171.6	171.0	2584.1	150	129	0.94	118	110	118	1.09	1.17	1.09
								250	168	1.21	159	135	159	1.05	1.24	1.05
								350	178	1.43	191	154	191	0.93	1.16	0.93
								550	229	1.79	239	180	222	0.96	1.27	1.03
$b_f=80; b_s=20; t=4.0mm$	$b_w=120$	1150	100	505	156.8	162.9	2675.7	150	128	0.96	116	106	116	1.10	1.21	1.10
								250	163	1.24	156	130	156	1.05	1.25	1.05
								350	184	1.47	186	148	186	0.99	1.25	0.99
								550	222	1.84	233	173	219	0.95	1.29	1.01
$b_f=106$	$b_w=106$	1150	95	495	194.0	177.4	2443.4	150	131	0.92	120	114	120	1.09	1.15	1.09
								250	176	1.19	162	141	162	1.09	1.25	1.09
								350	196	1.40	194	160	194	1.01	1.23	1.01
								550	233	1.76	244	187	228	0.96	1.24	1.02
$b_f=100; b_s=20; t=4.0mm$	$b_f=100$	2000	150	615	498.6	483.1	1647.3	150	149	0.56	150	150	150	0.99	0.99	0.99
								250	247	0.72	233	233	233	1.06	1.06	1.06
								350	342	0.85	296	287	296	1.16	1.19	1.16
								550	459	1.07	391	348	391	1.17	1.32	1.17
$b_f=90$	$b_f=90$	2000	145	570	504.6	530.6	1419.0	150	149	0.53	150	150	150	0.99	0.99	0.99
								250	248	0.69	238	238	238	1.04	1.04	1.04
								350	344	0.81	305	296	305	1.13	1.16	1.13
								550	480	1.02	407	362	407	1.18	1.33	1.18
$b_f=110$	$b_f=110$	2000	150	655	491.9	439.6	1867.8	150	149	0.58	150	150	150	1.00	1.00	1.00
								250	246	0.75	228	228	228	1.08	1.08	1.08
								350	332	0.89	286	277	286	1.16	1.20	1.16
								550	432	1.12	376	335	376	1.15	1.29	1.15
$b_s=15; b_f=85; t=2.4mm$	$b_s=15$	940	95	540	457.3	457.5	4246.8	150	148	0.57	150	150	150	0.99	0.99	0.99
								250	243	0.74	230	230	230	1.06	1.06	1.06
								350	325	0.87	290	276	290	1.12	1.18	1.12
								550	427	1.10	382	335	382	1.12	1.27	1.12
$b_s=13$	$b_s=13$	940	100	490	454.7	380.5	4156.3	150	148	0.63	148	148	148	1.00	1.00	1.00
								250	241	0.81	218	218	218	1.10	1.10	1.10
								350	305	0.96	271	259	271	1.12	1.18	1.12
								550	377	1.20	353	310	353	1.07	1.21	1.07
$b_s=17$	$b_s=17$	940	95	590	458.9	522.9	4337.9	150	148	0.54	150	150	150	0.99	0.99	0.99
								250	245	0.69	238	238	238	1.03	1.03	1.03
								350	332	0.82	304	288	304	1.09	1.15	1.09
								550	461	1.03	404	353	404	1.14	1.31	1.14
$b_w=100; b_s=5; t=1.0mm$	$b_f=50$	1400	80	270	104.1	105.1	777.9	150	101	1.19	97	82	97	1.04	1.23	1.04
								250	126	1.54	127	99	127	1.00	1.27	1.00
								350	151	1.82	149	112	149	1.01	1.35	1.01
								550	185	2.29	185	129	185	1.00	1.43	1.00
$b_f=45$	$b_f=45$	1400	80	250	105.2	116.3	653.5	150	107	1.14	101	86	101	1.06	1.25	1.06
								250	129	1.47	133	104	133	0.97	1.24	0.97
								350	151	1.73	157	117	157	0.96	1.29	0.96
								550	186	2.17	195	136	195	0.95	1.37	0.95
$b_f=55$	$b_f=55$	1400	85	290	102.8	95.0	903.2	150	97	1.26	92	79	92	1.05	1.23	1.05
								250	123	1.62	120	95	120	1.02	1.30	1.02
								350	145	1.92	142	106	142	1.02	1.37	1.02
								550	186	2.41	175	123	175	1.06	1.52	1.06

Table B2: Z columns – SFEA ultimate strengths and DSM estimates (dimensions in mm, stresses in MPa) – II

		GBT						SFEA		DSM						
	L	L _{crL}	L _{crD}	f _{crL}	f _{crD}	f _{crG}	f _y	f _U	λ _D	f _{ND}	f _{NDL}	f _{NL-D}	f _{U/f_{ND}}	f _{NDL/f_U}	f _{NL-D/f_U}	
<i>b_w=80; b_s=10; t=1.3mm</i>	<i>b_w=115</i>	2400	95	535	126.6	126.5	597.0	150	120	1.09	105	92	105	1.14	1.30	1.14
								250	131	1.41	139	112	139	0.95	1.17	0.95
								350	150	1.66	164	126	150	0.91	1.19	1.00
								550	177	2.09	204	147	184	0.87	1.20	0.96
								750	192	2.43	236	162	210	0.81	1.18	0.92
<i>b_w=80; b_s=10; t=0.95mm</i>	<i>b_w=100</i>	2400	90	530	136.8	129.5	533.4	150	125	1.08	106	94	106	1.18	1.32	1.18
								250	133	1.39	140	115	140	0.95	1.16	0.95
								350	151	1.64	166	130	150	0.91	1.17	1.00
								550	175	2.06	207	151	183	0.85	1.16	0.96
								750	189	2.41	239	166	209	0.79	1.14	0.91
<i>b_w=80; b_s=10; t=1.2mm</i>	<i>b_w=125</i>	2400	105	545	109.0	120.3	629.9	150	118	1.12	103	88	103	1.15	1.35	1.15
								250	130	1.44	135	106	135	0.96	1.22	0.96
								350	144	1.71	160	120	150	0.90	1.20	0.96
								550	165	2.14	199	139	184	0.83	1.18	0.90
								750	195	2.50	229	154	211	0.85	1.27	0.93
<i>b_w=95; b_s=80; t=0.95mm</i>	<i>b_s=10</i>	2500	85	610	93.8	98.7	468.2	150	100	1.23	94	78	94	1.06	1.27	1.06
								250	107	1.59	123	95	101	0.87	1.13	1.06
								350	114	1.88	145	106	115	0.79	1.07	0.99
								550	121	2.36	179	123	137	0.68	0.98	0.88
								750	163	2.76	206	135	154	0.79	1.20	1.06
<i>b_w=95; b_s=80; t=0.95mm</i>	<i>b_s=9</i>	2500	85	565	93.5	88.0	502.3	150	89	1.31	89	75	89	1.00	1.20	1.00
								250	101	1.69	116	90	99	0.87	1.13	1.02
								350	112	1.99	136	100	114	0.82	1.12	0.98
								550	126	2.50	168	116	137	0.75	1.09	0.92
								750	147	2.92	193	127	154	0.76	1.15	0.95
<i>b_w=95; b_s=10; t=1.2mm</i>	<i>b_s=11</i>	2500	85	650	94.0	106.3	473.5	150	111	1.19	97	81	97	1.14	1.37	1.14
								250	116	1.53	127	98	101	0.91	1.19	1.15
								350	124	1.81	150	110	114	0.83	1.13	1.09
								550	129	2.27	186	128	134	0.69	1.01	0.96
								750	149	2.66	214	141	149	0.70	1.06	1.00
<i>b_w=100; b_s=140; t=1.2mm</i>	<i>b_s=140</i>	1430	145	830	53.7	3753.8		150	67	1.67	70	54	64	0.96	1.25	1.06
								250	77	2.16	89	64	80	0.86	1.20	0.96
								350	105	2.55	104	71	92	1.01	1.48	1.14
								550	126	3.20	128	81	111	0.99	1.55	1.13
								750	148	3.74	146	89	126	1.01	1.66	1.17
<i>b_w=100; b_s=130; t=1.2mm</i>	<i>b_s=130</i>	1430	140	790	57.4	58.8	3514.6	150	62	1.60	73	57	67	0.84	1.08	0.92
								250	86	2.06	94	67	84	0.92	1.28	1.02
								350	102	2.44	110	75	98	0.93	1.36	1.05
								550	113	3.06	134	86	118	0.84	1.31	0.96
								750	131	3.57	154	95	134	0.85	1.38	0.98
<i>b_w=100; b_s=150; t=1.2mm</i>	<i>b_s=150</i>	1430	155	865	51.0	48.8	3966.8	150	58	1.75	67	51	61	0.87	1.15	0.95
								250	81	2.26	85	60	76	0.95	1.34	1.06
								350	97	2.68	99	67	88	0.98	1.45	1.10
								550	120	3.36	121	77	107	0.99	1.57	1.13
								750	145	3.92	139	84	121	1.05	1.73	1.20
<i>b_w=100; b_s=120.5; t=1.5mm</i>	<i>b_s=12.5</i>	1850	200	1105	46.0	46.0	4031.1	150	58	1.81	65	49	59	0.90	1.20	0.98
								250	72	2.33	82	57	74	0.88	1.26	0.97
								350	84	2.76	96	64	86	0.88	1.32	0.98
								550	117	3.46	117	73	103	1.00	1.60	1.13
								750	137	4.04	134	80	117	1.02	1.72	1.17
<i>b_w=100; b_s=14; t=1.5mm</i>	<i>b_s=14</i>	1850	195	1195	45.6	38.1	4058.6	150	58	1.98	59	44	52	0.98	1.30	1.11
								250	76	2.56	74	52	64	1.02	1.45	1.19
								350	91	3.03	86	58	73	1.05	1.58	1.24
								550	112	3.80	105	66	87	1.06	1.70	1.28
								750	133	4.44	120	72	99	1.11	1.85	1.35
<i>b_w=100; b_s=11; t=1.5mm</i>	<i>b_s=11</i>	1850	205	1010	46.5	52.5	4003.5	150	59	1.69	69	52	66	0.85	1.14	0.90
								250	76	2.18	88	61	83	0.86	1.24	0.92
								350	91	2.58	103	68	97	0.89	1.34	0.95
								550	116	3.24	126	78	117	0.92	1.48	0.99
								750	135	3.78	144	86	134	0.93	1.57	1.01

Table B3: Z columns – SFEA ultimate strengths and DSM estimates (dimensions in mm, stresses in MPa) – III

		GBT					SFEA		DSM							
	L	L _{crL}	L _{crD}	f _{crL}	f _{crD}	f _{crG}	f _y	f _U	λ _D	f _{ND}	f _{NDL}	f _{NL-D}	f _{U/f_{ND}}	f _{NDL/f_U}	f _{NL-D/f_U}	
<i>b_w=235; b_r=160; t=1.9mm</i>	<i>b_s=12.5</i>	1950	200	905	64.3	64.3	3489.5	150	73	1.53	77	60	75	0.95	1.20	0.97
			250	99	1.97	98	72	95	1.00	1.37	1.03	1.46	1.05	1.46	1.05	
			350	117	2.33	115	80	111	1.02	1.46	1.05	1.56	1.06	1.56	1.06	
			550	144	2.92	141	92	136	1.02	1.46	1.05	1.67	1.08	1.67	1.08	
			750	169	3.42	162	101	156	1.04	1.46	1.05	1.67	1.08	1.67	1.08	
<i>b_w=150; b_s=10; t=1.9mm</i>	<i>b_s=14</i>	1950	200	980	64.1	55.7	3526.5	150	72	1.64	71	57	68	1.01	1.27	1.05
			250	82	2.12	91	67	87	0.89	1.22	0.94	1.49	1.10	1.49	1.10	
			350	111	2.51	107	75	101	1.04	1.49	1.10	1.56	1.06	1.56	1.06	
			550	145	3.14	130	86	122	1.11	1.70	1.19	1.70	1.19	1.70	1.19	
			750	170	3.67	149	94	139	1.14	1.70	1.19	1.70	1.19	1.70	1.19	
<i>b_w=150; b_s=10; t=1.9mm</i>	<i>b_s=11</i>	1950	205	830	64.6	73.9	3452.1	150	84	1.42	82	64	82	1.02	1.30	1.02
			250	100	1.84	106	77	106	0.94	1.30	0.95	1.34	0.93	1.34	0.93	
			350	115	2.18	124	86	124	0.93	1.30	0.95	1.36	0.93	1.36	0.93	
			550	155	2.73	153	99	152	1.02	1.56	1.02	1.56	1.02	1.56	1.02	
			750	185	3.19	175	109	174	1.06	1.70	1.06	1.70	1.06	1.70	1.06	
<i>b_w=150; b_s=10; t=1.9mm</i>	<i>b_r=140</i>	900	150	800	63.5	63.5	9476.9	150	69	1.54	76	60	71	0.91	1.16	0.97
			250	91	1.98	98	71	90	0.93	1.27	1.01	1.36	1.03	1.36	1.03	
			350	108	2.35	114	80	104	0.94	1.36	1.03	1.40	1.03	1.40	1.03	
			550	137	2.94	140	91	127	0.98	1.50	1.08	1.50	1.08	1.50	1.08	
			750	161	3.44	161	100	144	1.00	1.61	1.01	1.61	1.01	1.61	1.01	
<i>b_w=150; b_s=10; t=1.9mm</i>	<i>b_r=130</i>	900	140	755	67.8	74.7	8872.9	150	76	1.42	82	65	82	0.92	1.16	0.92
			250	98	1.83	106	78	98	0.92	1.25	1.00	1.36	1.05	1.36	1.05	
			350	131	2.16	125	87	114	1.05	1.50	1.15	1.50	1.15	1.50	1.15	
			550	166	2.71	153	101	138	1.08	1.65	1.20	1.65	1.20	1.65	1.20	
			750	192	3.17	176	111	158	1.09	1.74	1.22	1.74	1.22	1.74	1.22	
<i>b_w=150; b_s=10; t=1.9mm</i>	<i>b_r=150</i>	900	155	835	58.2	58.2	10014.	150	70	1.61	73	57	68	0.96	1.23	1.03
			250	91	2.07	93	67	86	0.98	1.36	1.07	1.47	1.11	1.47	1.11	
			350	110	2.45	109	75	99	1.01	1.47	1.11	1.53	1.05	1.53	1.17	
			550	140	3.07	134	86	120	1.05	1.63	1.17	1.63	1.17	1.63	1.17	
			750	165	3.59	153	94	137	1.08	1.75	1.21	1.75	1.21	1.75	1.21	

Table B4: Z columns – SFEA ultimate strengths and DSM estimates (dimensions in mm, stresses in MPa) – IV

Appendix C

		GBT					SFEA			DSM						
		L	L _{crL}	L _{crD}	f _{crL}	f _{crD}	f _{crG}	f _y	f _U	λ _D	f _{ND}	f _{NLD}	f _{NL-D}	f _{U/ND}	f _{NDL/f_U}	f _{NL-D/f_U}
<i>b_w=180; b_s=10; b_f=21; t=1.5mm</i>	<i>b_f=70; b_s=20; b_f=60; t=1.2mm</i>	<i>b_w=150; b_s=20; b_f=60; t=1.2mm</i>	<i>b_f=70; b_s=20; b_f=32; t=1.2mm</i>	<i>b_w=80; b_f=50; b_s=25; t=1.0mm</i>	150	138	0.95	117	108	117	117	117	1.18	1.28	1.18	
					250	167	1.23	157	132	157	157	157	1.06	1.26	1.06	
					350	176	1.46	187	150	187	175	175	0.94	1.17	0.94	
					550	183	1.83	235	175	175	175	175	0.78	1.04	1.04	
					750	184	2.13	272	194	194	194	194	0.68	0.95	0.95	
					150	131	1.02	111	102	111	111	111	1.18	1.28	1.18	
					250	154	1.32	147	125	147	147	147	1.05	1.23	1.05	
					350	165	1.56	175	141	141	141	141	0.94	1.17	1.17	
					550	179	1.95	219	164	164	164	164	0.82	1.09	1.09	
					750	186	2.28	253	182	182	182	182	0.74	1.02	1.02	
<i>b_w=180; b_s=10; b_f=21; t=2.4mm</i>	<i>b_f=70; b_s=20; b_f=32; t=1.2mm</i>	<i>b_w=150; b_s=20; b_f=60; t=1.2mm</i>	<i>b_f=70; b_s=20; b_f=60; t=1.2mm</i>	<i>b_w=80; b_f=50; b_s=25; t=1.0mm</i>	150	141	0.94	118	109	118	118	118	1.19	1.29	1.19	
					250	173	1.21	159	134	159	159	159	1.09	1.29	1.09	
					350	182	1.43	191	152	191	191	191	0.95	1.19	0.95	
					550	190	1.79	239	178	178	178	178	0.79	1.06	1.06	
					750	191	2.09	277	198	198	198	198	0.69	0.97	0.97	
					150	135	1.00	113	102	113	113	113	1.20	1.32	1.20	
					250	157	1.29	151	125	151	151	151	1.04	1.25	1.04	
					350	169	1.52	179	142	142	142	142	0.94	1.19	1.19	
					550	175	1.91	224	165	165	165	165	0.78	1.06	1.06	
					750	186	2.23	259	183	183	183	183	0.72	1.02	1.02	
<i>b_w=100; b_s=20; b_f=60; t=1.2mm</i>	<i>b_f=70; b_s=20; b_f=32; t=1.2mm</i>	<i>b_w=150; b_s=20; b_f=60; t=1.2mm</i>	<i>b_f=70; b_s=20; b_f=60; t=1.2mm</i>	<i>b_w=80; b_f=50; b_s=25; t=1.0mm</i>	150	134	1.04	109	97	109	109	109	1.23	1.38	1.23	
					250	155	1.34	145	119	145	145	145	1.07	1.31	1.07	
					350	166	1.59	172	134	134	134	134	0.96	1.24	1.24	
					550	179	1.99	215	156	156	156	156	0.83	1.15	1.15	
					750	182	2.32	248	173	173	173	173	0.73	1.05	1.05	
					150	79	1.47	79	63	79	79	79	1.00	1.25	1.00	
					250	100	1.90	102	75	75	75	75	0.98	1.33	1.33	
					350	120	2.25	120	84	84	84	84	1.00	1.43	1.43	
					550	142	2.82	147	97	97	97	97	0.97	1.47	1.47	
					750	154	3.30	168	106	106	106	106	0.91	1.45	1.45	
<i>b_w=90; b_s=10; b_f=21; t=1.5mm</i>	<i>b_f=70; b_s=20; b_f=32; t=1.2mm</i>	<i>b_w=150; b_s=20; b_f=60; t=1.2mm</i>	<i>b_f=70; b_s=20; b_f=60; t=1.2mm</i>	<i>b_w=80; b_f=50; b_s=25; t=1.0mm</i>	150	82	1.45	80	64	80	80	80	1.02	1.27	1.02	
					250	105	1.88	104	77	77	77	77	1.01	1.37	1.37	
					350	110	2.22	121	86	86	86	86	0.91	1.28	1.28	
					550	124	2.78	149	99	99	99	99	0.83	1.26	1.26	
					750	126	3.25	171	108	108	108	108	0.74	1.16	1.16	
					150	71	1.54	76	60	60	60	60	0.93	1.17	1.17	
					250	91	1.99	97	72	72	72	72	0.93	1.27	1.27	
					350	101	2.36	114	80	80	80	80	0.89	1.26	1.26	
					550	117	2.95	140	92	92	92	92	0.84	1.27	1.27	
					750	117	3.45	160	101	101	101	101	0.73	1.16	1.16	
<i>b_w=115; b_s=10; b_f=21; t=1.5mm</i>	<i>b_f=70; b_s=20; b_f=32; t=1.2mm</i>	<i>b_w=150; b_s=20; b_f=60; t=1.2mm</i>	<i>b_f=70; b_s=20; b_f=60; t=1.2mm</i>	<i>b_w=80; b_f=50; b_s=25; t=1.0mm</i>	150	82	1.43	82	66	82	82	82	1.00	1.24	1.00	
					250	92	1.85	105	79	79	79	79	0.87	1.17	1.05	
					350	100	2.19	123	88	88	88	88	0.81	1.14	1.01	
					550	107	2.74	152	101	118	118	118	0.71	1.06	0.91	
					750	107	3.21	174	111	133	133	133	0.62	0.96	0.81	
					150	83	1.37	85	69	85	85	85	0.97	1.20	0.97	
					250	99	1.77	110	82	94	94	94	0.89	1.20	1.05	
					350	106	2.09	129	92	108	108	108	0.82	1.15	0.99	
					550	111	2.62	159	106	129	129	129	0.70	1.05	0.86	
					750	114	3.06	183	117	146	146	146	0.62	0.98	0.78	
<i>b_w=130; b_s=10; b_f=21; t=1.5mm</i>	<i>b_f=70; b_s=20; b_f=32; t=1.2mm</i>	<i>b_w=150; b_s=20; b_f=60; t=1.2mm</i>	<i>b_f=70; b_s=20; b_f=60; t=1.2mm</i>	<i>b_w=80; b_f=50; b_s=25; t=1.0mm</i>	150	79	1.50	78	63	78	78	78	1.01	1.26	1.01	
					250	91	1.93	101	75	82	82	82	0.90	1.21	1.10	
					350	99	2.29	118	84	94	94	94	0.84	1.18	1.05	
					550	106	2.87	145	96	111	111	111	0.73	1.10	0.95	
					750	109	3.35	166	106	125	125	125	0.66	1.03	0.87	
					150	147	0.76	136	136	136	136	136	1.08	1.08	1.08	
					250	229	0.98	191	174	191	191	191	1.20	1.31	1.20	
					350	266	1.16	232	200	232	232	232	1.14	1.33	1.14	
					550	289	1.45	296	237	296	296	296	0.98	1.22	0.98	
					750	301	1.69	346	265	265	265	265	0.87	1.14	1.14	
<i>b_w=85; b_f=75; b_s=15; b_f=20; t=1.2mm</i>	<i>b_f=70; b_s=20; b_f=32; t=1.2mm</i>	<i>b_w=150; b_s=20; b_f=60; t=1.2mm</i>	<i>b_f=70; b_s=20; b_f=60; t=1.2mm</i>	<i>b_w=80; b_f=50; b_s=25; t=1.0mm</i>	150	144	0.87	125	119	125	125	1.15	1.21	1.15		
					250	191	1.12	170	147	170	170	170	1.12	1.30	1.12	
					350	203	1.33	205	168	205	205	205	0.99	1.21	0.99	
					550	215	1.66	258	197	197	197	197	0.83	1.09	1.09	
					750	224	1.94	300	219	219	219	219	0.75	1.02	1.02	

Table C1: R columns – SFEA ultimate strengths and DSM estimates (dimensions in mm, stresses in MPa) – I

Table C2: R columns – SFEA ultimate strengths and DSM estimates (dimensions in mm, stresses in MPa) – II

		GBT					SFEA		DSM							
		L	L _{crL}	L _{crD}	f _{crL}	f _{crD}	f _{crG}	f _y	f _U	λ _D	f _{ND}	f _{NLD}	f _{ND-D}	f _{U/f_{ND}}	f _{ND/f_U}	f _{ND-D/f_U}
$b_w=75; b_f=75; b_s=15; t=1.0mm$	$b_w=55; b_s=15; b_f=20; t=1.2mm$	$b_w=75; b_f=60; b_s=20; t=1.2mm$	$b_w=75; b_f=75; b_s=15; t=1.2mm$	150	143	0.89	123	114	123	1.16	1.25	1.16				
								250	184	1.15	167	142	167	1.10	1.30	1.10
								350	197	1.36	201	162	201	0.98	1.22	0.98
								550	224	1.70	253	190	190	0.89	1.18	1.18
								750	241	1.98	293	211	211	0.82	1.14	1.14
	$b_w=60; b_s=20; t=1.2mm$	$b_w=75; b_f=60; b_s=20; t=1.2mm$	$b_w=75; b_f=75; b_s=15; t=1.2mm$	150	146	0.82	130	120	130	1.13	1.21	1.13				
								250	204	1.06	178	151	178	1.14	1.35	1.14
								350	221	1.26	215	173	215	1.03	1.28	1.03
								550	239	1.58	272	204	204	0.88	1.17	1.17
								750	239	1.84	317	227	227	0.75	1.05	1.05
$b_w=80; b_s=15; b_f=20; t=1.2mm$	$b_w=55; b_s=15; b_f=20; t=1.2mm$	$b_w=75; b_f=60; b_s=20; t=1.2mm$	$b_w=75; b_f=75; b_s=15; t=1.2mm$	150	137	0.95	117	109	117	1.17	1.26	1.17				
								250	165	1.23	157	134	157	1.05	1.23	1.05
								350	186	1.46	187	152	187	0.99	1.23	0.99
								550	219	1.83	235	177	177	0.93	1.23	1.23
								750	212	2.13	272	196	196	0.78	1.08	1.08
	$b_w=70; b_s=20; t=1.2mm$	$b_w=75; b_f=60; b_s=20; t=1.2mm$	$b_w=75; b_f=75; b_s=15; t=1.2mm$	150	147	0.72	140	140	140	1.05	1.05	1.05				
								250	229	0.93	199	185	199	1.15	1.24	1.15
								350	267	1.10	243	213	243	1.10	1.25	1.10
								550	303	1.38	311	254	311	0.97	1.19	0.97
								750	336	1.61	365	283	283	0.92	1.19	1.19
$b_w=85; b_s=15; b_f=20; t=1.2mm$	$b_w=60; b_s=20; t=1.2mm$	$b_w=75; b_f=60; b_s=20; t=1.2mm$	$b_w=75; b_f=75; b_s=15; t=1.2mm$	150	147	0.72	140	140	140	1.05	1.05	1.05				
								250	230	0.93	199	190	199	1.16	1.21	1.16
								350	271	1.10	243	219	243	1.11	1.24	1.11
								550	321	1.38	311	260	311	1.03	1.24	1.03
								750	347	1.61	365	290	290	0.95	1.20	1.20
	$b_w=75; b_s=20; t=1.2mm$	$b_w=75; b_f=60; b_s=20; t=1.2mm$	$b_w=75; b_f=75; b_s=15; t=1.2mm$	150	146	0.73	139	139	139	1.05	1.05	1.05				
								250	228	0.94	196	178	196	1.16	1.28	1.16
								350	262	1.12	240	205	240	1.09	1.28	1.09
								550	296	1.40	306	244	306	0.97	1.21	0.97
								750	330	1.63	358	272	272	0.92	1.21	1.21
$b_w=80; b_s=15; b_f=20; t=1.2mm$	$b_w=55; b_s=15; b_f=20; t=1.2mm$	$b_w=75; b_f=60; b_s=20; t=1.2mm$	$b_w=75; b_f=75; b_s=15; t=1.2mm$	150	146	0.76	136	136	136	1.08	1.08	1.08				
								250	222	0.99	190	172	190	1.17	1.29	1.17
								350	248	1.17	230	197	230	1.08	1.26	1.08
								550	284	1.46	293	233	293	0.97	1.22	0.97
								750	303	1.71	342	260	260	0.88	1.16	1.16
	$b_w=70; b_s=20; t=1.2mm$	$b_w=75; b_f=60; b_s=20; t=1.2mm$	$b_w=75; b_f=75; b_s=15; t=1.2mm$	150	144	0.83	129	129	129	1.12	1.12	1.12				
								250	201	1.07	177	161	177	1.13	1.25	1.13
								350	227	1.27	214	184	214	1.06	1.23	1.06
								550	273	1.59	270	217	217	1.01	1.26	1.26
								750	288	1.86	315	241	241	0.92	1.20	1.20
$b_w=85; b_s=15; b_f=20; t=1.2mm$	$b_w=60; b_s=20; t=1.2mm$	$b_w=75; b_f=60; b_s=20; t=1.2mm$	$b_w=75; b_f=75; b_s=15; t=1.2mm$	150	147	0.73	139	139	139	1.06	1.06	1.06				
								250	230	0.94	197	178	197	1.17	1.30	1.17
								350	264	1.11	240	204	240	1.10	1.29	1.10
								550	296	1.40	307	243	307	0.96	1.22	0.96
								750	317	1.63	359	272	272	0.88	1.17	1.17
	$b_w=70; b_s=20; t=1.2mm$	$b_w=75; b_f=60; b_s=20; t=1.2mm$	$b_w=75; b_f=75; b_s=15; t=1.2mm$	150	145	0.83	129	125	129	1.12	1.16	1.16				
								250	205	1.07	177	157	177	1.16	1.31	1.16
								350	223	1.27	214	179	214	1.04	1.25	1.04
								550	247	1.59	271	211	211	0.91	1.17	1.17
								750	264	1.85	315	234	234	0.84	1.13	1.13
$b_w=85; b_s=15; b_f=20; t=1.2mm$	$b_w=70; b_s=20; t=1.2mm$	$b_w=75; b_f=60; b_s=20; t=1.2mm$	$b_w=75; b_f=75; b_s=15; t=1.2mm$	150	145	0.84	128	123	128	1.13	1.18	1.13				
								250	199	1.08	175	154	175	1.13	1.30	1.13
								350	215	1.28	212	175	212	1.02	1.23	1.02
								550	234	1.61	267	206	206	0.88	1.13	1.13
								750	255	1.88	311	230	230	0.82	1.11	1.11
	$b_w=75; b_s=20; t=1.2mm$	$b_w=75; b_f=60; b_s=20; t=1.2mm$	$b_w=75; b_f=75; b_s=15; t=1.2mm$	150	146	0.81	131	128	131	1.11	1.14	1.11				
								250	211	1.04	182	161	182	1.16	1.31	1.16
								350	230	1.23	220	184	220	1.05	1.25	1.05
								550	262	1.54	278	217	217	0.94	1.21	1.21

Table C3: R columns – SFEA ultimate strengths and DSM estimates (dimensions in mm, stresses in MPa) – III

Appendix D

		GBT					SFEA		DSM							
	L	L _{crL}	L _{crD}	f _{cr,L}	f _{cr,D}	f _{cr,G}	f _y	f _u	λ _D	f _{ND}	f _{NDL}	f _{NL-D}	f _{U/f_{ND}}	f _{NDL/f_U}	f _{NL-D/f_U}	
<i>b_w=100; b_r=10; t=2.4mm</i>	<i>b_r=55</i>	620	85	310	583.6	564.2	4305.6	150	149	0.52	150	150	150	0.99	0.99	0.99
			250	245	0.67	241	241	241	1.01	1.01	1.01	1.01	1.01	1.01	1.01	
			350	335	0.79	311	311	311	1.08	1.08	1.08	1.08	1.08	1.08	1.08	
			550	456	0.99	417	382	417	1.09	1.09	1.20	1.09	1.20	1.09	1.09	
<i>b_w=180; b_r=10; t=1.9mm</i>	<i>b_r=50</i>	620	80	290	591.0	589.9	4110.1	150	149	0.50	150	150	150	0.99	0.99	0.99
			250	246	0.65	243	243	243	1.01	1.01	1.01	1.01	1.01	1.01	1.01	
			350	338	0.77	315	315	315	1.07	1.07	1.07	1.07	1.07	1.07	1.07	
			550	473	0.97	424	389	424	1.12	1.12	1.22	1.12	1.22	1.12	1.12	
<i>b_w=180; b_r=10; t=1.9mm</i>	<i>b_r=60</i>	620	85	325	579.2	529.3	4460.7	150	149	0.53	150	150	150	0.99	0.99	0.99
			250	244	0.69	238	238	238	1.02	1.02	1.02	1.02	1.02	1.02	1.02	
			350	329	0.81	305	305	305	1.08	1.08	1.08	1.08	1.08	1.08	1.08	
			550	440	1.02	406	372	406	1.08	1.08	1.18	1.08	1.18	1.08	1.08	
<i>b_w=180; b_r=10; t=1.9mm</i>	<i>b_r=110</i>	1030	150	590	112.7	112.7	4808.0	150	104	1.15	100	86	100	1.04	1.21	1.04
			250	132	1.49	131	104	131	1.01	1.01	1.27	1.01	1.27	1.01	1.01	
			350	156	1.76	155	117	155	1.01	1.01	1.33	1.01	1.33	1.01	1.01	
			550	195	2.21	192	136	192	1.02	1.02	1.44	1.02	1.44	1.02	1.02	
<i>b_w=180; b_r=10; t=1.9mm</i>	<i>b_r=130</i>	1030	160	650	108.5	98.8	5116.1	150	97	1.23	94	81	94	1.03	1.20	1.03
			250	122	1.59	123	97	122	0.99	0.99	1.25	1.00	1.25	1.00	1.00	
			350	145	1.88	145	109	144	1.00	1.00	1.33	1.01	1.33	1.01	1.01	
			550	184	2.36	179	126	178	1.03	1.03	1.46	1.03	1.46	1.03	1.03	
<i>b_w=180; b_r=10; t=1.9mm</i>	<i>b_r=90</i>	1030	145	515	116.0	131.6	4306.6	150	116	1.07	107	92	107	1.09	1.26	1.09
			250	147	1.38	141	112	141	1.04	1.04	1.31	1.04	1.31	1.04	1.04	
			350	175	1.63	168	126	168	1.04	1.04	1.38	1.04	1.38	1.04	1.04	
			550	223	2.04	208	147	208	1.07	1.07	1.51	1.07	1.51	1.07	1.07	
<i>b_w=110; b_r=10; t=1.9mm</i>	<i>b_s=17.5</i>	1760	105	755	261.5	261.5	823.2	150	145	0.76	136	136	136	1.06	1.06	1.06
			250	198	0.98	191	174	191	1.04	1.04	1.14	1.04	1.14	1.04	1.04	
			350	239	1.16	232	200	232	1.03	1.03	1.20	1.03	1.20	1.03	1.03	
			550	283	1.45	296	237	296	0.96	0.96	1.19	0.96	1.19	0.96	0.96	
<i>b_w=110; b_r=10; t=1.9mm</i>	<i>b_s=20</i>	1760	105	830	262.7	284.2	863.5	150	147	0.73	139	139	139	1.05	1.05	1.05
			250	229	0.94	197	180	197	1.16	1.16	1.28	1.16	1.28	1.16	1.16	
			350	290	1.11	241	207	241	1.20	1.20	1.40	1.20	1.40	1.20	1.20	
			550	323	1.39	308	246	308	1.05	1.05	1.31	1.05	1.31	1.05	1.05	
<i>b_w=110; b_r=10; t=1.9mm</i>	<i>b_s=16</i>	1760	105	710	261.1	238.6	801.0	150	143	0.79	133	133	133	1.08	1.08	1.08
			250	190	1.02	184	168	184	1.03	1.03	1.13	1.03	1.13	1.03	1.03	
			350	232	1.21	223	192	223	1.04	1.04	1.21	1.04	1.21	1.04	1.04	
			550	271	1.52	283	227	246	0.96	0.96	1.19	0.96	1.19	1.10	1.10	
<i>b_w=80; b_r=10; t=1.0mm</i>	<i>b_w=95</i>	2500	85	595	103.8	103.6	273.3	150	95	1.20	96	82	96	0.99	1.16	0.99
			250	112	1.55	126	99	106	0.89	0.89	1.14	1.05	1.14	1.05	1.05	
			350	125	1.84	148	111	122	0.84	0.84	1.13	1.03	1.13	1.03	1.03	
			550	138	2.30	183	128	145	0.75	0.75	1.08	0.95	1.08	0.95	0.95	
<i>b_w=80; b_r=10; t=1.0mm</i>	<i>b_w=88</i>	2500	85	590	114.6	106.7	240.4	150	95	1.19	97	84	97	0.98	1.13	0.98
			250	116	1.53	127	102	109	0.91	0.91	1.14	1.06	1.14	1.06	1.06	
			350	125	1.81	151	114	125	0.83	0.83	1.09	1.00	1.09	1.00	1.00	
			550	135	2.27	186	133	149	0.72	0.72	1.02	0.90	1.02	0.90	0.90	
<i>b_w=80; b_r=10; t=1.0mm</i>	<i>b_w=105</i>	2500	90	605	88.9	93.4	321.9	150	93	1.27	92	76	92	1.01	1.22	1.01
			250	100	1.64	119	91	101	0.84	0.84	1.10	0.99	1.10	0.99	0.99	
			350	118	1.94	141	102	116	0.84	0.84	1.15	1.01	1.15	1.01	1.01	
			550	136	2.43	173	118	139	0.78	0.78	1.15	0.98	1.15	0.98	0.98	

Table D1: C columns – SFEA ultimate strengths and DSM estimates (dimensions in mm, stresses in MPa) – I

		GBT					SFEA		DSM							
	L	L _{crL}	L _{crD}	f _{crL}	f _{crD}	f _{crG}	f _y	f _U	λ _D	f _{ND}	f _{NDL}	f _{NL-D}	f _{U/f_{ND}}	f _{NDL/f_U}	f _{NL-D/f_U}	
<i>b_f=80; b_s=10; t=1.5mm</i>	<i>b_w=114</i>	1150	100	500	171.6	170.8	1725.3	150	126	0.94	118	110	118	1.06	1.15	1.06
								250	166	1.21	159	135	159	1.04	1.23	1.04
								350	189	1.43	191	153	191	0.99	1.23	0.99
								550	221	1.79	239	180	226	0.93	1.23	0.98
								750	254	2.10	277	199	260	0.92	1.28	0.98
<i>b_w=180; b_s=20; t=4.0mm</i>	<i>b_f=120</i>	1150	100	505	156.8	165.9	1867.1	150	125	0.95	117	107	117	1.07	1.17	1.07
								250	162	1.23	157	131	157	1.03	1.23	1.03
								350	183	1.45	188	149	188	0.97	1.23	0.97
								550	221	1.82	235	174	221	0.94	1.27	1.00
								750	255	2.13	273	193	255	0.94	1.32	1.00
<i>b_w=106</i>	<i>b_f=106</i>	1150	90	495	194.0	177.0	1537.3	150	128	0.92	120	114	120	1.07	1.12	1.07
								250	172	1.19	162	141	162	1.06	1.22	1.06
								350	198	1.41	194	160	194	1.02	1.24	1.02
								550	207	1.76	243	187	224	0.85	1.11	0.92
								750	260	2.06	282	207	257	0.92	1.25	1.01
<i>b_w=180; b_s=20; t=4.0mm</i>	<i>b_f=100</i>	2000	150	620	498.8	482.2	1398.2	150	149	0.56	150	150	150	0.99	0.99	0.99
								250	239	0.72	233	233	233	1.02	1.02	1.02
								350	283	0.85	296	286	296	0.96	0.99	0.96
								550	361	1.07	391	348	391	0.92	1.04	0.92
								750	430	1.25	465	393	465	0.92	1.09	0.92
<i>b_w=110; b_s=85; t=2.4mm</i>	<i>b_f=90</i>	2000	145	580	504.8	526.3	1335.3	150	149	0.53	150	150	150	0.99	0.99	0.99
								250	245	0.69	238	238	238	1.03	1.03	1.03
								350	305	0.82	304	295	304	1.00	1.03	1.00
								550	377	1.02	405	361	405	0.93	1.04	0.93
								750	442	1.19	484	409	484	0.91	1.08	0.91
<i>b_w=110; b_s=5; t=1.0mm</i>	<i>b_f=110</i>	2000	150	660	492.0	438.8	1446.4	150	149	0.58	150	150	150	1.00	1.00	1.00
								250	225	0.75	228	228	228	0.99	0.99	0.99
								350	266	0.89	286	277	286	0.93	0.96	0.93
								550	349	1.12	375	334	375	0.93	1.04	0.93
								750	418	1.31	445	377	445	0.94	1.11	0.94
<i>b_w=110; b_s=15; t=2.4mm</i>	<i>b_f=15</i>	940	95	545	457.4	457.5	2702.1	150	148	0.57	150	150	150	0.99	0.99	0.99
								250	239	0.74	230	230	230	1.04	1.04	1.04
								350	304	0.87	290	276	290	1.05	1.10	1.05
								550	398	1.10	382	335	382	1.04	1.19	1.04
								750	459	1.28	454	378	454	1.01	1.21	1.01
<i>b_w=110; b_s=13; t=2.4mm</i>	<i>b_f=13</i>	940	100	495	454.7	379.7	2606.7	150	148	0.63	148	148	148	1.00	1.00	1.00
								250	232	0.81	218	218	218	1.06	1.06	1.06
								350	287	0.96	271	258	271	1.06	1.11	1.06
								550	380	1.20	352	310	352	1.08	1.23	1.08
								750	434	1.41	416	348	416	1.04	1.25	1.04
<i>b_w=110; b_s=17; t=2.4mm</i>	<i>b_f=17</i>	940	95	595	459.0	498.2	2806.7	150	148	0.55	150	150	150	0.99	0.99	0.99
								250	243	0.71	235	235	235	1.03	1.03	1.03
								350	320	0.84	299	284	299	1.07	1.13	1.07
								550	434	1.05	396	346	396	1.10	1.25	1.10
								750	491	1.23	472	392	472	1.04	1.25	1.04
<i>b_w=110; b_s=55; t=1.0mm</i>	<i>b_f=50</i>	1400	80	270	104.1	105.2	716.9	150	103	1.19	97	82	97	1.06	1.25	1.06
								250	133	1.54	127	99	127	1.05	1.34	1.05
								350	159	1.82	149	112	149	1.06	1.42	1.06
								550	191	2.29	185	129	185	1.03	1.48	1.03
								750	197	2.67	213	143	213	0.92	1.38	0.92
<i>b_w=110; b_s=45; t=2.4mm</i>	<i>b_f=45</i>	1400	80	250	105.2	116.6	665.2	150	108	1.13	101	86	101	1.07	1.26	1.07
								250	137	1.46	133	104	133	1.03	1.31	1.03
								350	168	1.73	158	117	158	1.07	1.43	1.07
								550	205	2.17	195	136	195	1.05	1.50	1.05
								750	223	2.54	225	150	225	0.99	1.48	0.99
<i>b_w=110; b_s=55; t=1.0mm</i>	<i>b_f=55</i>	1400	85	290	102.8	95.0	759.2	150	99	1.26	92	79	92	1.07	1.26	1.07
								250	116	1.62	120	95	120	0.96	1.23	0.96
								350	155	1.92	142	106	142	1.09	1.46	1.09
								550	189	2.41	175	123	175	1.08	1.54	1.08
								750	207	2.81	201	135	201	1.03	1.53	1.03

Table D2: C columns – SFEA ultimate strengths and DSM estimates (dimensions in mm, stresses in MPa) – II

		L	GBT					SFEA		DSM						
			L _{crL}	L _{crD}	f _{crL}	f _{crD}	f _{crG}	f _y	f _U	λ _D	f _{ND}	f _{NLD}	f _{U/f_{ND}}	f _{NLD/f_U}	f _{NLD-f_U}	
$b_w=80; b_f=80; t=1.3mm$	$b_w=115$	2400	95	540	126.6	126.2	405.2	150	108	1.09	105	92	105	1.03	1.17	1.03
								250	134	1.41	138	112	138	0.97	1.20	0.97
								350	145	1.67	164	126	150	0.88	1.15	0.97
								550	161	2.09	204	147	183	0.79	1.10	0.88
								750	176	2.44	235	162	209	0.75	1.09	0.84
$b_w=95; b_f=80; t=0.95mm$	$b_w=100$	2400	90	530	136.8	129.1	324.7	150	109	1.08	106	94	106	1.03	1.16	1.03
								250	138	1.39	140	115	140	0.99	1.20	0.99
								350	150	1.65	166	129	150	0.90	1.16	1.00
								550	165	2.06	206	151	183	0.80	1.10	0.90
								750	179	2.41	238	166	208	0.75	1.08	0.86
$b_w=125$	$b_w=125$	2400	105	545	109.0	119.9	459.4	150	105	1.12	102	87	102	1.02	1.20	1.02
								250	128	1.44	135	106	135	0.95	1.20	0.95
								350	140	1.71	160	120	149	0.88	1.17	0.94
								550	160	2.14	198	139	183	0.81	1.15	0.87
								750	176	2.50	229	154	210	0.77	1.15	0.84
$b_w=150; b_f=10; t=1.2mm$	$b_s=10$	2500	85	610	93.8	94.1	273.0	150	91	1.26	92	77	92	0.99	1.18	0.99
								250	106	1.63	120	93	99	0.89	1.15	1.07
								350	111	1.93	141	104	113	0.79	1.07	0.98
								550	130	2.42	174	120	134	0.75	1.08	0.97
								750	145	2.82	200	132	150	0.72	1.10	0.97
$b_w=150; b_f=9; t=1.2mm$	$b_s=9$	2500	85	570	93.5	87.8	268.3	150	88	1.31	89	75	89	0.98	1.18	0.98
								250	100	1.69	116	90	99	0.86	1.11	1.01
								350	106	2.00	136	100	113	0.78	1.06	0.93
								550	130	2.50	168	116	136	0.78	1.12	0.96
								750	146	2.92	193	127	153	0.76	1.15	0.96
$b_w=150; b_f=11; t=1.2mm$	$b_s=11$	2500	85	655	94.0	100.0	278.1	150	101	1.22	95	79	95	1.07	1.28	1.07
								250	111	1.58	123	95	98	0.90	1.17	1.14
								350	131	1.87	146	107	110	0.90	1.23	1.19
								550	144	2.35	180	124	129	0.80	1.16	1.12
								750	152	2.74	207	136	143	0.73	1.12	1.06
$b_w=140; b_f=140; t=1.2mm$	$b_f=140$	1430	145	835	53.7	54.1	1969.7	150	61	1.67	70	54	64	0.86	1.12	0.95
								250	80	2.15	90	64	80	0.89	1.25	1.00
								350	97	2.54	105	71	92	0.93	1.36	1.05
								550	123	3.19	128	82	111	0.96	1.51	1.11
								750	145	3.72	147	89	126	0.99	1.62	1.15
$b_w=140; b_f=130; t=1.2mm$	$b_f=130$	1430	140	795	57.4	59.8	1949.9	150	64	1.58	74	57	68	0.86	1.11	0.94
								250	83	2.04	95	68	85	0.88	1.22	0.98
								350	100	2.42	111	76	98	0.90	1.31	1.02
								550	127	3.03	136	87	119	0.94	1.46	1.07
								750	149	3.54	155	95	135	0.96	1.56	1.11
$b_w=150; b_f=150; t=1.2mm$	$b_f=150$	1430	155	870	58.7	48.7	1983.0	150	61	1.76	67	52	61	0.91	1.16	0.99
								250	78	2.27	85	62	77	0.92	1.27	1.02
								350	94	2.68	99	69	88	0.94	1.36	1.06
								550	119	3.36	121	78	107	0.98	1.52	1.12
								750	139	3.92	138	86	121	1.00	1.62	1.15
$b_w=200; b_f=190; t=1.5mm$	$b_s=12.5$	1850	200	1105	46.1	46.1	2304.3	150	58	1.80	65	49	59	0.89	1.18	0.97
								250	76	2.33	82	57	74	0.92	1.31	1.02
								350	89	2.76	96	64	86	0.93	1.40	1.04
								550	114	3.45	117	73	103	0.97	1.56	1.10
								750	133	4.03	134	80	118	0.99	1.66	1.13
$b_w=200; b_f=190; t=1.5mm$	$b_s=14$	1850	195	1200	45.6	38.1	2104.5	150	55	1.98	59	44	52	0.94	1.25	1.07
								250	74	2.56	74	52	64	1.00	1.42	1.16
								350	88	3.03	86	58	73	1.02	1.53	1.21
								550	112	3.80	105	66	87	1.06	1.70	1.28
								750	132	4.44	120	72	98	1.10	1.83	1.34
$b_w=200; b_f=190; t=1.5mm$	$b_s=11$	1850	205	1010	46.5	52.5	2068.7	150	59	1.69	69	52	66	0.85	1.14	0.90
								250	77	2.18	88	61	83	0.87	1.25	0.92
								350	91	2.58	103	68	97	0.89	1.34	0.95
								550	115	3.24	126	78	117	0.91	1.47	0.98
								750	134	3.78	144	86	134	0.93	1.56	1.00

Table D3: C columns – SFEA ultimate strengths and DSM estimates (dimensions in mm, stresses in MPa) – III

		L	GBT					SFEA		DSM						
			L _{crL}	L _{crD}	f _{crL}	f _{crD}	f _{crG}	f _y	f _U	λ _D	f _{ND}	f _{NDL}	f _{NL-D}	f _{U/f_{ND}}	f _{NDL/f_U}	f _{NL-D/f_U}
<i>b_w=235; b_r=160; t=1.9mm</i>	<i>b_s=12.5</i>	1950	200	910	64.4	64.4	2378.7	150	74	1.53	77	61	75	0.96	1.22	0.99
								250	94	1.97	99	72	95	0.96	1.31	0.99
								350	112	2.33	115	80	111	0.97	1.39	1.01
								550	144	2.92	141	92	136	1.02	1.56	1.06
<i>b_w=150; b_s=10; t=1.9mm</i>	<i>b_s=14</i>	1950	200	985	64.1	55.7	2401.8	150	73	1.64	71	57	68	1.02	1.29	1.07
								250	92	2.12	91	67	86	1.00	1.37	1.06
								350	110	2.51	107	75	100	1.03	1.48	1.10
								550	142	3.14	130	86	122	1.09	1.66	1.16
<i>b_w=150; b_s=10; t=1.9mm</i>	<i>b_s=11</i>	1950	205	830	64.6	74.0	2357.0	150	77	1.42	82	64	82	0.94	1.19	0.94
								250	97	1.84	106	77	106	0.92	1.26	0.92
								350	113	2.17	124	86	124	0.91	1.31	0.91
								550	143	2.73	153	99	152	0.94	1.44	0.94
<i>b_w=150; b_s=10; t=1.9mm</i>	<i>b_r=140</i>	900	150	800	63.5	63.5	4970.4	150	71	1.54	76	60	71	0.93	1.18	0.99
								250	94	1.98	98	71	90	0.97	1.32	1.05
								350	113	2.35	114	80	104	0.99	1.42	1.08
								550	145	2.94	140	91	127	1.03	1.59	1.14
<i>b_w=150; b_s=10; t=1.9mm</i>	<i>b_r=130</i>	900	140	760	67.8	71.4	4920.3	150	75	1.45	81	64	81	0.93	1.17	0.93
								250	100	1.87	104	76	95	0.96	1.30	1.04
								350	119	2.21	122	85	111	0.98	1.39	1.08
								550	152	2.78	150	98	134	1.02	1.55	1.13
<i>b_w=150; b_s=10; t=1.9mm</i>	<i>b_r=150</i>	900	155	835	58.2	58.2	5004.5	150	67	1.61	73	57	68	0.92	1.19	0.99
								250	88	2.07	93	67	86	0.94	1.30	1.02
								350	108	2.45	109	75	99	0.99	1.44	1.09
								550	138	3.07	134	86	120	1.03	1.60	1.15

Table D4: C columns – SFEA ultimate strengths and DSM estimates (dimensions in mm, stresses in MPa) – IV